Technical Report

DSWA-TR-98-2

RADIATION ENVIRONMENT PROGRAM (REP) 1992 TO 1994

Approved for public release; distribution is unlimited.

September 2000

Prepared for:
Defense Threat Reduction Agency
45045 Aviation Drive
Dulles, VA 20166-7517

DNA001-92-C-0082

Dean C. Kaul
Stephen D. Egbert

Prepared by: Science Applications International Corporation
10260 Campus Point Drive
San Diego, CA 92121

DESTRUCTION NOTICE:

Destroy this report when it is no longer needed. Do not return to sender.

PLEASE NOTIFY THE DEFENSE THREAT REDUCTION AGENCY, ATTN: ADM, 45045 AVIATION DRIVE, DULLES, VA 20166-7517, IF YOUR ADDRESS IS INCORRECT, IF YOU WISH IT DELETED FROM THE DISTRIBUTION LIST, OR IF THE ADDRESSEE IS NO LONGER EMPLOYED BY YOUR ORGANIZATION.

CUT HERE AND RETURN

DISTRIBUTION LIST UPDATE

This mailer is provided to enable DTRA to maintain current distribution lists for reports. (We would appreciate you providing the requested information.)

- ☐ Add the individual listed to your distribution list.
- ☐ Delete the cited organization/individual.
- ☐ Change of address.

Note:
Please return the mailing label from the document so that any additions, changes, corrections or deletions can be made easily. For distribution cancellation or more information call DTRA/ADM (703) 325-1036.

NAME: _____

ORGANIZATION: _____

OLD ADDRESS	NEW ADDRESS
_____	_____
_____	_____
_____	_____

TELEPHONE NUMBER: ( ) _____

DTRA PUBLICATION NUMBER/TITLE	CHANGES/DELETIONS/ADDITIONS, etc.) *(Attach Sheet if more Space is Required)*
_____	_____
_____	_____
_____	_____

DTRA or other GOVERNMENT CONTRACT NUMBER: _____

CERTIFICATION of NEED-TO-KNOW BY GOVERNMENT SPONSOR (if other than DTRA):

SPONSORING ORGANIZATION: _____

CONTRACTING OFFICER or REPRESENTATIVE: _____

SIGNATURE: _____

DEFENSE THREAT REDUCTION AGENCY
ATTN: ADM
45045 AVIATION DRIVE
DULLES, VA 20156-7517

DEFENSE THREAT REDUCTION AGENCY
ATTN: ADM
6801 TELEGRAPH ROAD
ALEXANDRIA, VA 22310-3398

REPORT DOCUMENTATION PAGE	Form Approved OMB No. 0704-0188

1. AGENCY USE ONLY (*Leave blank*)	2. REPORT DATE	3. REPORT TYPE AND DATES COVERED
		Technical 920324 - 971031

4. TITLE AND SUBTITLE

Radiation Environment Program (REP) 1992 to 1994

5. FUNDING NUMBERS

C - DNA 001-92-C-0082
PE - 4662D
PR - RM
TA - AD
WU - DH00009

6. AUTHOR(S)

Dean C. Kaul and Stephen D. Egbert

7. PERFORMING ORGANIZATION NAME(S) AND ADDRESS(ES)

Science Applications International Corporation
10260 Campus Point Drive
San Diego, CA 92121

8. PERFORMING ORGANIZATION REPORT

SAIC-98/1000

9. SPONSORING/MONITORING AGENCY NAME(S) AND ADDRESS(ES)

Defense Threat Reduction Agency
45045 Aviation Drive
Dulles, VA 20166-7517

CPWB/Kehlet

10. SPONSORING/MONITORING AGENCY REPORT NUMBER

DSWA-TR-98-2

11. SUPPLEMENTARY NOTES

This work was sponsored by the Defense Threat Reduction Agency under RDT&E RMC code B 4662 D RM AD 00009 3500 A AF 25904D.

12a. DISTRIBUTION/AVAILABILITY STATEMENT

Approved for public release; distribution is unlimited.

12B. DISTRIBUTION CODE

13. ABSTRACT (Maximum 200 words)

This is a report of radiation transport computations by Science Applications International Corporation (SAIC), under contract to the Defense Special Weapons Agency (DSWA). It describes efforts to verify and validate the MASH shielding system and its associated DABL69 (ENDF/B-V) cross section set. The report describes MASH calculations of free field fluence and kerma intended to match neutron and gamma ray fluence and dose measurements mad at Aberdeen Pulse Radiation Facility (APRF). It describes the technical approach taken in performing the calculations, as well as a detailed comparison between calculation and measurements made at APRF between the spring of 1992 and the Fall of 1994, which marked the end of the REP program. Calculations include those using the standard MASH package and those involving revisions and perturbations to the MASH calculations, incorporating new cross section data and new applications of MASH technology. These additions specifically account for forest in the vicinity of a measurement sire and examine the affect of revised cross sections, in order to understand and explain discrepancies between calculation and measurement.

14. SUBJECT TERMS		15. NUMBER OF PAGES
Ionizing Radiation	Nucleus Weapons	
Neutron	Cross Sections	16. PRICE CODE
Gamma Ray	Monte Carlo	

17. SECURITY CLASSIFICATION OF THIS PAGE	18. SECURITY CLASSIFICATION OF REPORT	19. SECURITY CLASSIFICATION OF ABSTRACT	20. LIMITATION OF ABSTRACT
UNCLASSIFIED	UNCLASSIFIED	UNCLASSIFIED	SAR

CLASSIFIED BY:

N/A since Unclassified

DECLASSIFY ON:

N/A since Unclassified

14. SUBJECT TERMS (Continued)

MASH
Discrete Ordinates
Computer Codes

PREFACE

The authors would like to thank the leader of the Radiation Environments Program, Mr. Rob Kehlet and all of the participants, measurers and calculators, from the United States and its NATO allies who made this program possible and brought it to a satisfactory and productive conclusion.

CONVERSION TABLE

Conversion factors for U.S. Customary to metric (SI) units of measurement.

MULTIPLY TO GET	BY	TO GET DIVIDE
angstrom	1.000 000 X E −10	meters (m)
atmosphere	1.013 25 X E +2	kilo pascal (kPa)
bar	1.000 000 X E +2	kilo pascal (kPa)
barn	1.000 000 X E -28	meter^2 (m^2)
British thermal unit (themochemical)	1.054 350 X E +3	joule (J)
calorie (themochemical)	4.184 000	joule (J)
cal (thermochemical/cm^2)	4.184 000 X E -2	mega joule/m^2 (MJ/m^2)
curie	3.700 000 X E +1	*giga becquerel (GBq)
degree (angle)	1.745 329 X E -2	radian (rad)
degree Fahrenheit	$t_k = (t^\circ f + 459.67)/1.8$	degree kelvin (K)
electron volt	1.602 19 X E -19	joule (J)
erg	1.000 000 X E -7	joule (J)
erg/second	1.000 000 X E -7	watt (W)
foot	3.048 000 X E -1	meter (m)
foot-pound-force	1.355 818	joule (J)
gallon (U.S. liquid)	3.785 412 X E -3	meter^3 (m^3)
inch	2.540 000 X E -2	meter (m)
jerk	1.000 000 X E +9	joule (J)
joule/kilogram (J/kg) radiation dose absorbed	1.000 000	Gray (Gy)
kilotons	4.183	terajoules
kip (1000 lbf)	4.448 222 X E +3	newton (N)
kip/inch^2 (ksi)	6.894 757 X E +3	kilo pascal (kPa)
ktap	1.000 000 X E +2	newton-second/m2 (N-s/m^2)
micron	1.000 000 X E -6	meter (m)
mil	2.540 000 X E -5	meter (m)
mile (international)	1.609 344 X E +3	meter (m)
ounce	2.834 952 X E -2	kilogram (kg)
pound-force (lbs avoirdupois)	4.448 222	newton (N)
pound-force inch	1.129 848 X E -1	newton-meter (N m)
pound-force/inch	1.751 268 X E +2	newton/meter (N/m)
pound-force/foot^2	4.788 026 X E -2	kilo pascal (kPa)
pound-force/inch^2 (psi)	6.894 757	kilo pascal (kPa)
pound-mass (lbm avoirdupois)	4.535 924 X E -1	kilogram (kg)
pound-mass-foot^2 (moment of inertia)	4.214 011 X E -2	kilogram-meter^2 (kg m^2)
pound-mass/foot^3	1.601 846 X E +1	kilogram/meter^3 (kg/m^3)
rad (radiation dose absorbed)	1.000 000 X E -2	**Gray (Gy)
roentgen	2.579 760 X E -4	coulomb/kilogram (C/kg)
shake	1.000 000 X E -8	second (s)
slug	1.459 390 X E +1	kilogram (kg)
torr (mm Hg, O° C)	1.333 22 X E -1	kilo pascal (kPa)

*The becquerel (Bq) is the SI unit of radioactivity; 1 Bq = 1 event/s.
**The Gray (Gy) is the SI unit of absorbed radiation.

TABLE OF CONTENTS

Section			Page
	PREFACE		**iii**
	CONVERSION TABLE		**iv**
	FIGURES		**vi**
	TABLES		**xv**
1	**INTRODUCTION**		**1**
2	**FREE FIELD CALCULATIONS AND COMPARISON WITH EXPERIMENTS**		**2**
	2.1	CALCULATIONAL APPROACH	7
	2.2	COMPARISON BETWEEN CALCULATIONS AND MEASUREMENTS	11
	2.2.1	Gold Foil Activation (APRF)	11
	2.2.2	Chlorine Transmutation (LLNL)	14
	2.2.3	Bf3 measurements (APRF)	14
	2.2.4	Sulfur Activation (APRF)	16
	2.2.5	Remmeter Measurements (APRF)	17
	2.2.6	Proton Recoil (ROSPEC) Measurements (APRF, DREO)	18
	2.2.7	Boron-Loaded Plastic Scintillator (LANL)	19
	2.2.8	Bonner Ball Measurements (EML)	19
	2.2.9	Thermoluminescent Dosimetry (APRF)	22
	2.2.10	Geiger Counter Gamma Ray Measurements (APRF)	24
3	**MODIFICATIONS TO CALCULATIONS**		**25**
	3.1	EFFECTS OF CALCULATION MODIFICATIONS AT 170 AND 400 METERS	25
	3.2	THE EFFECT OF THE FOREST AT 715 METERS	28
	3.3	CORRECTED CALCULATION COMPARISON WITH MEASUREMENTS	31
4	LUCITE PHANTOM SHIELDING CALCULATIONS		35
5	CONCLUSIONS AND RECOMMENDATIONS		38
6	REFERENCES		39
Appendix			
A	**REACTOR RUNS, METEOROLOGICAL AND SURFACE CONDITIONS, 1992-1994 MEASUREMENT SERIES**		**A-1**
	A.1	REACTOR RUNS	A-1
	A.2	METEOROLOGICAL CONDITIONS	A-2
	A.3	GROUND MOISTURE CONDIITONS	A-3
B	**MEASURED AND CALCULATED FLUENCE, 1992-1994 MEASUREMENT SERIES**		**B-1**
	DISTRIBUTION LIST		**DL -1**

FIGURES

Figure		Page
2-1	Ground surface elevation above sea level of source and measurement locations at APRF	2
2-2	Gold foil activation (cadmium difference) calculation to measurement ratio	12
2-3	Gold foil activation cadmium ration calculation to measurement ratio	12
2-4	Thermal neutron height effect as measured by gold foils	13
2-5	Thermal neutron height effect as calculated for gold foils	13
2-6	Chlorine foil transmutation, calculation to measurement ratio for thermal neutron fluence	14
2-7	Bare Bf3 neutron response	15
2-8	Bf3 (cadmium difference) calculation to measurement ratio	15
2-9	Sulfur activation calculation to measurement ratio	16
2-10	Neutron doses & dose equivalents as measured by remmeter, calculation to measurement ratio	17
2-11	Proton Recoil (ROSPEC) neutron doses calculation to measurement ratio	18
2-12	Boron-Loaded Plastic Scintillator dose and fluence (>3 MeV) calculation to measurement ratios	19
2-13	Bonner Ball neutron dose calculation to measurement ratio	20
2-14	Bonner Ball greater than 3 MeV neutron fluence calculation to measurement ratio	21
2-15	Bonner Ball neutron fluence spectra calculation to measurement ratio	21
2-16	CaF2 TLD gamma ray dose calculation to measurement ratio	22
2-17	LiF TLD gamma ray dose calculation to measurement ratio	23
2-18	A1203 TLD gamma ray dose calculation to measurement ratio	23
2-19	Geiger Counter, gamma ray dose calculation to measurement ratio	24
3-1	Factors for correcting MASH calculated neutron fluence at 170 m for ENDF/B-6 cross sections, non-uniform terrain and forest	25
3-2	Factors for correcting MASH calculated neutron fluence at 400 m for ENDF/B-6 cross sections, non-uniform terrain and forest	26
3-3	Factors for correcting MASH calculated gamma ray fluence at 170 m for non-uniform terrain and forest	27

FIGURES (Continued)

Figure		Page
3-4	Factors for correcting MASH calculated gamma ray fluence at 400 m for non-uniform terrain and forest	27
3-5	715-meter measurement site, neutron fluence corrections due to surrounding forest	30
3-6	715-meter measurement site, gamma ray fluence corrections due to surrounding forest	30
3-7	Sulfur activation calculation to measurement ratio, as calculated (left) and corrected (right)	31
3-8	Neutron doses and dose equivalents as measured by remmeter, calculation to measurement ratio, as calculated (left) and corrected (right)	32
3-9	Proton recoil (ROSPEC) neutron doses calculation to measurement ratio, calculation to Measurement ratio, as calculated (left) and corrected (right)	32
3-10	Bonner Ball neutron dose calculation to measurement ratio, as calculated (left) and corrected (right)	33
3-11	Bonner Ball greater than 3 MeV neutron fluence calculation to measurement ratio, as calculated (left) and corrected (right)	33
3-12	Boron-loaded plastic Scintillator dose and fluence (>3 MeV) calculation to measurement ratio, as calculated (left) and corrected (right)	34
4-1	Neutron fluence distributions, front to back, in a cylindrical Lucite phantom	36
4-2	Neutron fluence in a Lucite phantom, calculation to measurement ratios	37
B-1	Neutron fluence, run SS92-228 at 170 m distance, uncorrected (left) and corrected (right)	B-1
B-2	Neutron fluence, runs SS92-232 and 233 at 400 m distance, uncorrected (left) and corrected (right)	B-2
B-3	Neutron fluence, Run SS92-240 at 715 m distance (on road), uncorrected (left) and corrected (right)	B-2
B-4	Neutron fluence, 1080 meters	B-3
B-5	Neutron fluence, 1600 meters	B-4

TABLES

Table		Page
2-1	APRF site geometry	3
2-2	List of measurement devices, spectrometers and dosimeters, used in the 1992-1994 series	4
2-3	Listing of reactor runs performed with passive dosimetry	5
2-4	Listing of reactor runs performed with active dosimetry	6
2-5	1990 revised neutron and gamma ray leakage per kw-hr from the APRF fast reactor, 1 hour operation	9
2-6	Element constituents of air, borated concrete and ground	10
3-1	Element constituents used in forest perturbation calculations	29
4-1	Lucite phantom elemental constituents	35

SECTION 1
INTRODUCTION

The armed forces of the United States, particularly the U.S. Army, require verified analytical models, methods and associated calculated data, which are validated for use in nuclear weapon initial radiation shielding, dosimetry analysis, targeting, operational planning and in vulnerability and effects assessment. The Radiation Environment Program (REP) is intended to develop and test the requisite hardware, software and data and make them available for use by the Department of Defense and its contractors.

Under the REP program, Government Fiscal Years 1987 to 1994, Science Applications International Corporation (SAIC) and Oak Ridge National Laboratory tested the MASH shielding analysis system [4]. This was done by comparing data calculated using MASH with those obtained from measurements of free field kerma and fluence performed at the Aberdeen Pulse Radiation Facility (APRF) and reporting the results of those tests [6,8]. The fast reactor at APRF, deployed outdoors, produces fluences of neutrons and gamma rays, which bear a strong resemblance to those from a tactical nuclear fission weapon. In the process of performing this comparison SAIC also examined a variety of factors affecting its quality, including the effect of updated radiation reaction cross sections, and the effect of forest in the vicinity of measurement sites.

This is a report of computations performed by Science Applications International Corporation (SAIC), performed under contract to the Defense Special Weapons Agency (DSWA). It is arranged to emphasize the efforts to verify and validate the MASH shielding system and its associated DABL (ENDF/B-V) cross section set. Thus, Section 2 of this report describes MASH calculations of free field fluence and kerma intended to match measurements made at APRF. That section contains a description of the technical approach taken in performing the calculations, as well as a detailed comparison between calculation and measurements made at APRF between the Spring of 1992 and the Fall of 1994, which marked the end of the REP program.

Section 3 of this report describes revisions and perturbations to the MASH calculations presented in Section 2. Some of these modifications are not part of the standard MASH package, but represent efforts to incorporate new cross section data and new applications of MASH technology, specifically accounting for large areas of forest in the vicinity of a measurement site. This is done in order to better understand and explain discrepancies between calculation and measurement.

Section 4 describes measurements and associated MASH shielding calculations associated with dose and fluence distributions in a cylindrical lucite phantom.

Section 5 provides a summary of findings discussed elsewhere in the body of the report. Appendix A to the report also provides detailed information on the atmospheric and surface conditions at APRF during the 1992 - 1994 experiments series. Appendix B provides comparisons of detailed calculated and measured spectra over a large range of distances.

SECTION 2
FREE FIELD CALCULATIONS AND COMPARISON WITH EXPERIMENTS

Between 23 October 1992 and 3 November 1994 a series of measurements of neutron and gamma ray kerma and fluence were performed at the Army Pulse Radiation Facility (APRF), using the fast reactor as a radiation source. The purpose of these measurements was to perform an inter-comparison of results from a variety of techniques, as well as to provide data against which to test the results of calculations performed using the MASH shielding system[4] and its component codes. Primarily, these are the two-dimensional, discrete ordinates transport system, DOS, and the three-dimensional, Monte Carlo transport code MORSE.

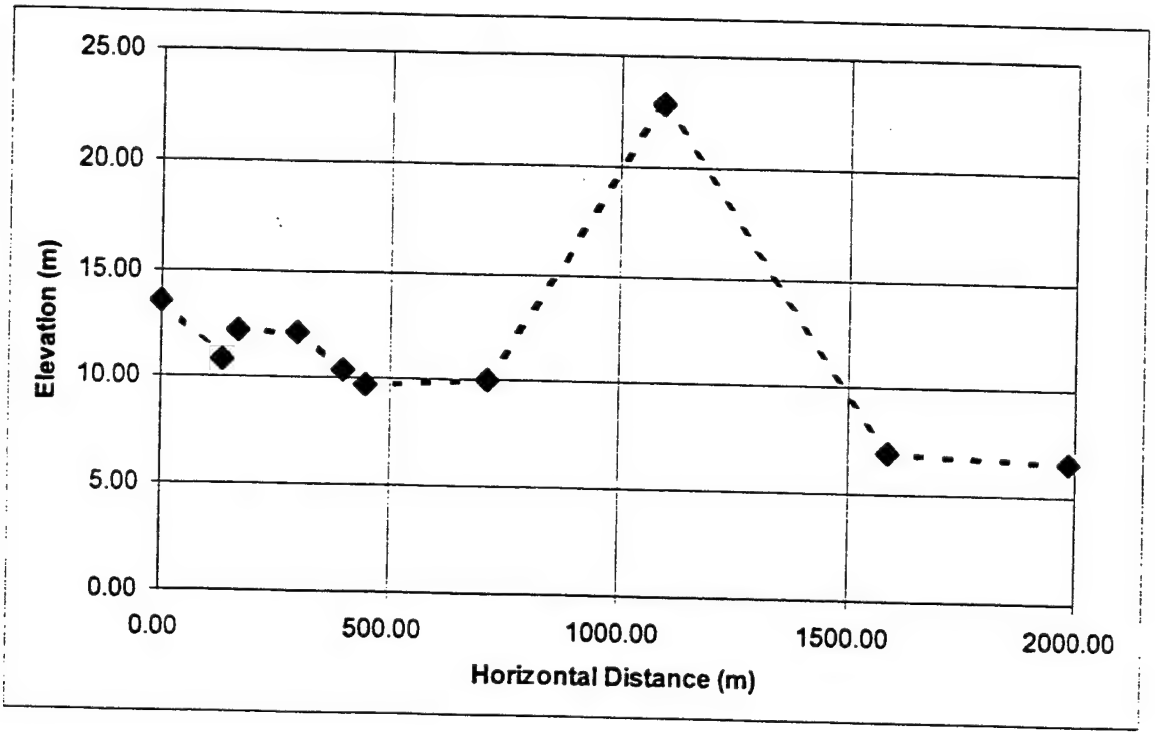

Figure 2-1. Ground surface elevation above sea level of source and measurement locations at APRF.

Measurements were performed at distances from 135 meters to 1986 meters from the reactor, which was deployed outside its environmental containment and raised to a height of 12.7 meters above a borated concrete pad, having an elevation of 13.58 meters, as given in Table 2-1 and illustrated in Figure 2-1. The measurements were performed in the free field, 1.5 meters above terrain, which varied somewhat in elevation from that at the reactor location.

Participants in the measurements included APRF[3], Defense Research Establishment Ottawa (DREO, Canada)[3], Los Alamos National Laboratory (LANL)[1], Lawrence Livermore Laboratory (LLNL, USA)[9] and Environmental Measurements Laboratory (EML, USA)[2], which performed measurements with a variety of dosimeters and spectrometers. These are listed in Table 2, along with the applicable energy range for each.

Table 2-1. APRF Site Geometry [3].

Location	North Coord. meters	East Coord. meters	Horizontal Distance meters	Elevation meters	Reactor Height meters
X Cut	4364779.48	396554.64	0	13.58	12.70
135 meter Position	4364889.11	396475.86	135.00	10.82	15.46
170 meter Position	4364917.53	396455.44	170.00	12.23	14.05
300 meter Position	4365023.11	396379.58	300.00	12.12	14.16
400 meter Position	4365104.32	396321.23	400.00	10.40	15.88
450 meter Position	4365144.92	396292.06	450.00	9.70	16.58
715 meter Position	4365360.13	396137.42	715.00	10.04	16.24
Aluminum Stake	4365530.18	396153.50	851.16	10.04	16.24
Pt. 1	4364960.55	396558.70	181.12	10.07	16.21
Pt. 2	4364819.28	396607.59	66.24	9.46	16.82
Pt. 3	4364728.20	396591.86	63.36	7.83	18.45
Pt. 4	4364741.50	396504.88	62.60	9.24	17.04
Pt. 5	4364669.84	396633.41	135.00	5.78	20.50
Pt. 6	4364700.70	396445.00	135.00	7.80	18.48
Hub & Tack Set-Top of Mound	4365720.42	395997.32	1093.61	22.81	3.48
Hub & Tack Set @ 1500 meters	4365605.47	397911.43	1588.44	6.98	19.30
Hub & Tack Set @ 2000 meters	4365289.23	398474.45	1986.34	6.58	19.70

Table 2-2. List of measurement devices, spectrometers and dosimeters, used in the 1992 - 1994 series [3].

APRF

Gold Activation (Cadmium Difference)
En < 0.414 eV[a]
Sulfur Activation
En > 3 MeV
Bf3 Proportional Counter (Cadmium Difference)
En < 0.414 eV
ROSPEC Rotating, Multi-stage Hydrogen Proportional Counter (Spectrometer)
56.6 keV < En < 4.51 MeV
Thermoluminescent Dosimeters
10 keV < Eγ < 20 MeV
Geiger-Mueller Counter (Dosimeter)
10 keV < Eγ < 20 MeV

DREO

ROSPEC Rotating, Multi-stage Hydrogen Proportional Counter (Spectrometer)
56.6 keV < En < 4.51 MeV

EML

Bonner Spheres (Spectrometer)
0.414 eV < En < 20 MeV

LANL

Boron-Loaded Plastic Scintillator
400 keV < En < 20 MeV

LLNL

Chlorine Activation
En < 0.414 eV

aEnergy ranges applicable to reported data.

Table 2-3. Listing of reactor runs performed with passive dosimetry [3].

Horiz. Distance/Angle meters/degrees	Measurement Device: Neutron			Gamma Ray
	Sulfur	Gold(Cd)	Chlorine	TLD
Run No.:	Date:		Energy:	
SS92-66	3/24/92		50 kwhr	
135/0	X	X	X	X
135/90	X	X	X	X
135/180	X	X	X	X
170	X	X	X	X
300	X	X	X	X
400	X	X	X	X
450	X	X	X	X
715	X	X	X	X
Run No.:	Date:		Energy:	
SS92-186	6/17/92		12 kwhr	
70/90	X	X		X
70/180	X	X		X
70/270	X	X		X
135/0	X	X		X
135/90	X	X		X
135/180	X	X		X
170	X	X		
In-Silo	X	X		X
Run No.:	Date:		Energy:	
SS92-210	7/7/92		50 kwhr	
135/0	X	X	X	
170	X	X	X	
300	X	X	X	
400	X	X	X	
450	X		X	
Run No.:	Date:		Energy:	
SS92-73	6/15/93		1 kwhr	
SS92-74	6/15/93		30 kwhr	
SS92-75	6/16/93		16 kwhr	
Acrylic phantom				

Table 2-4. Listing of reactor runs performed with active dosimetry [3].

Dates: 5/27/92 to 5/29/92
Horiz. Distance/Angle Measurement Device: Run No. SS92-:

meters/degrees	APRF Neutron			Gamma Ray	Total	DOE Neutron
	BF3	Gold(Cd)	Sulfur	GM	REM	Bon. Sph.
135		157	157			
170	155	154	154	155	155	
170		157	157			
300		157	157			
400	156	154	154		156	
400		157	157			
450		157	157			
715	158			158	158	158
1080	154			154	154	157
1600	154			154	154	154
2000	157			157	157	157

Dates: 8/25/92 to 9/2/92
Horiz. Distance/Angle Measurement Device: Run No. SS92-:

meters/degrees	APRF Neutron		DREO Neutron		Gamma Ray
	BF3	ROSPEC	BF3	ROSPEC	BGO
70/180			239	239	
135/0	230	230	230	230	
135/180	239	239			
170	228	228	228	228	
170	229	229	229	229	
300		236	236		
300	237	237	237		
400	231	231	231	231	
400	232	232	232	232	
400	233				
400				242	
450	234	234			
450	235			235	
715	240	240	240	240	
715	241				
715		241		241	
silo	238	238	238	238	
1600					240

Table 2-4. Listing of reactor runs performed with active dosimetry. (Continued)

Dates:	6/14/93 to 6/17/93				
Horiz. Distance/Angle	Measurement Device:		Run No. SS93-:		
	APRF Neutron				EML Neutron
meters/degrees	BF3	ROSPEC	Gamma Ray GM	Total REM	Bon. Sph.
300	71		71	71	71
300	72		72	72	72
300	73	73			
1600	77		77	77	77
2000	74		74	74	74
2000	75		75	75	75
2000	76		76	76	76
2000			73		

Dates:	6/14/93 to 6/17/93	
Horiz. Distance/Angle	Measurement Device:	Run No. SS95-:
	LANL Neutron	
meters/degrees		
1080	33	
1600	34	

2.1 CALCULATIONAL APPROACH.

Calculations of neutron and gamma ray kerma and fluence were performed to compare with each of the measurement series. The calculations were performed using the MASH code system, taking into account the atmospheric and surface conditions that existed at the time of each experiment. Appendix A of this report contains a listing of the experiments, associated run numbers and the meteorological and surface conditions existing over the duration of each.

The APRF radiation environment was calculated using the DOS module, GRTUNCL, to determine the uncollided components of the fluences propagating from the neutron and gamma ray sources and the associated first-collision sources. The DORT module of DOS was used to calculate the scattered and secondary fluence components, using the spatially-distributed, neutron and gamma ray first-collision sources. The use of the first-collision sources was necessary to avoid streaming along quadrature angles, a calculational artifact referred to as a "ray effect."

SAIC performed calculations using a geometry model incorporating air, ground and a borated concrete pad directly below the reactor. The model was a simple depiction of the APRF site, with the reactor represented by a point source over flat ground. The height of the point source was 14 meters above the borated concrete pad, which is the traditional value used to depict the altitude of the APRF source and is very close to 14.36 meters, which is the effective height for eight locations at which measurements have been made 135, 170, 300, 400, 450, 750, 1588 and 1986 meters. The flat-ground model extended to a radius of 2325 m, using 101 intervals, and to a height of 1280 m, using 75 intervals, of which 58 were in the air and 17 were in one meter of ground. The first few meshes near the ground are centered at 5, 17, 37, 70, 125, and 220 cm above the ground.

All calculations used a point source, differential in energy and angle. The scalar neutron and gamma ray source spectra are given in Table 2-5. That source was calculated by SAIC, published in 1989 and revised in 1990 [5,6]. The source and cross section energy format was that of the DABL, ENDF/B-V cross section set (46neutron/23gamma ray). The angle quadrature was a 240 angle set, derived from a symmetric S8 quadrature by subdividing each angle five for one in the polar direction. The purpose of the subdivision of polar angles was to reduce quadrature streaming (ray effects) in the secondary gamma ray component. Ray effects in that component result from the creation of a very intense, localized source of secondary gamma rays in the ground below the source and are not reduced through the use of a first collision source. The cross sections were implemented using a P5 legendre scattering order.

ENDF/B-V cross sections are a part of the MASH 1.0 system. Elemental kerma factors were taken from Kerr [7] and other sources.

Table 2-5. 1990 revised neutron and gamma ray leakage per kw-hr from the APRF fast reactor, 1 hour operation [6].

GROUP NO.	UPPER ENERGY (MeV)	NEUTRON LEAKAGE
1	1.964E+01	3.60E+11
2	1.691E+01	1.41E+12
3	1.492E+01	1.63E+12
4	1.419E+01	1.19E+12
5	1.384E+01	9.18E+12
6	1.252E+01	3.68E+12
7	1.221E+01	2.76E+13
8	1.105E+01	5.94E+13
9	1.000E+01	1.15E+14
10	9.048E+00	2.05E+14
11	8.187E+00	3.36E+14
12	7.408E+00	8.57E+14
13	6.376E+00	2.69E+15
14	4.966E+00	7.66E+14
15	4.724E+00	2.82E+15
16	4.066E+00	8.16E+15
17	3.012E+00	8.56E+15
18	2.385E+00	1.37E+15
19	2.307E+00	1.01E+15
20	1.827E+00	1.19E+16
21	1.423E+00	1.27E+16
22	1.108E+00	7.02E+15
23	9.616E - 01	7.77E+15
24	8.209E - 01	4.53E+15
25	7.427E - 01	6.94E+15
26	6.393E - 01	6.52E+15
27	5.502E - 01	1.36E+16
28	3.688E - 01	9.53E+15
29	2.472E - 01	6.23E+15
30	1.576E - 01	2.86E+15
31	1.111E - 01	2.45E+15
32	5.248E - 02	5.65E+14
33	3.431E - 02	1.06E+14
34	2.479E - 02	5.93E+13
35	2.188E - 02	1.22E+14
36	1.033E - 02	3.30E+13
37	3.355E - 03	4.98E+12
38	1.234E - 03	4.48E+11
39	5.830E - 04	6.31E+10
40	2.754E - 04	1.49E+10
41	1.013E - 04	2.46E+09
42	2.902E - 05	3.16E+08
43	1.068E - 05	5.93E+07
44	3.059E - 06	8.66E+06
45	1.125E - 06	1.50E+06
46	4.140E - 07	2.38E+05
LOWER BOUND	1.000E - 11	
Total:		1.29E+17
Gamma Ray Leakage		
1	2.00E+01	2.34E+09
2	1.40E+01	1.14E+10
3	1.20E+01	5.07E+11
4	1.00E+01	1.61E+13
5	8.00E+00	2.37E+13
6	7.00E+00	6.00E+13
7	6.00E+00	2.34E+14
8	5.00E+00	6.00E+14
9	4.00E+00	1.93E+15
10	3.00E+00	2.04E+15
11	2.50E+00	3.44E+15
12	2.00E+00	5.74E+15
13	1.50E+00	1.04E+16
14	1.00E+00	9.50E+15
15	7.00E - 01	8.61E+15
16	4.50E - 01	4.07E+15
17	3.00E - 01	3.12E+15
18	1.50E - 01	5.70E+14
19	1.00E - 01	6.92E+13
20	7.00E - 02	2.89E+12
21	4.50E - 02	8.10E+10
22	3.00E - 02	9.38E+09
23	2.00E - 02	3.07E+10
LOWER BOUND	1.00E - 02	
Total:		5.04E+16

Table 2-6. Elemental constituents of air, borated concrete and ground.

Elemental Densities (atoms per barn-centimeter)

	Air			Ground			
Run	240	241	66	240/241		66	
				10%H2O	25%H2O	33%H2O	50%H2O
				> 500 m	< 500 m	> 500 m	< 500 m
H	7.35-7*	9.36-7	1.33-7	9.88-3	2.47-2	3.26-2	4.94-2
C				1.66-3	1.66-3	1.66-3	1.66-3
N	3.78-5	3.81-5	4.08-5	5.19-5	5.19-5	5.19-5	5.19-5
O	1.09-5	1.11-5	1.15-5	3.28-2	4.02-2	4.42-2	5.26-2
Na				1.57-4	1.57-4	1.57-4	1.57-4
Mg				1.00-4	1.00-4	1.00-4	1.00-4
Al				1.51-3	1.51-3	1.51-3	1.51-3
Si				1.06-2	1.06-2	1.06-2	1.06-2
P				0.0	0.0	0.0	0.0
S				3.83-6	3.83-6	3.83-6	3.83-6
Cl				3.76-6	3.76-6	3.76-6	3.76-6
Ar	2.26-7	2.28-7	2.44-7				
K				2.25-4	2.25-4	2.25-4	2.25-4
Ca				1.28-3	1.28-3	1.28-3	1.28-3
Mn				8.01-6	8.01-6	8.01-6	8.01-6
Fe				3.52-4	3.52-4	3.52-4	3.52-4
Cu				5.32-7	5.32-7	5.32-7	5.32-7

aRead as $7.35*10^{-7}$

The flat-ground calculation was run using the air, borated concrete and ground elemental constituents given in Table 2-6. That table contains the description of ground including 25% moisture by dry weight.

SAIC determined the radiation environments applicable to each measurement series by performing calculations for each time at which meteorological data were reported, usually at half hour intervals, within the temporal bounds of each experiment interval and taking the mean. Meteorological values selected for use were those corresponding to sea level. The ground moisture content was measured at an array of locations at the beginning of the experiment series, as described in the Appendix. For the purposes of the calculations it was assumed to be uniform over the ground surface in two regions, differing within and without a radius of 500 meters, as shown in Table 2-6.

2.2 COMPARISON BETWEEN CALCULATIONS AND MEASUREMENTS.

This section of the report contains a comparison of calculation and measurement results. The calculations referred to in this section were made using the MASH system, including DABL69 (DLC-130) cross sections, assuming a flat earth geometry. No corrections are made for the presence of forest or terrain anomalies or for the effect of more modern cross section data. Those corrections and their effects are described in Section 3 of this report.

2.2.1 Gold Foil Activation (APRF).

Measurements and calculations were made for two gold foil sizes. The small foils were circular, 1.11 cm diameter by 0.0127 cm thick, approximately 0.25 g each. The large foils were rectangular, 2.54 cm by 4.45 cm, and 0.0127 cm thick, each having a mass of approximately 2.5 g. The cadmium covers were 0.051 cm and 0.0254 cm thick for the small and large foils, respectively. The large foils were placed 100 cm above the ground. The small foils were placed at heights of 10, 100, 300 and 3000 cm.

Figure 2-2 shows the gold foil activation, cadmium difference ($E_n < 0.414$ eV) calculation to measurement ratios for the small and large foils. Both calculation and measurement results depict the effective 2200 meter/second fluence. The calculations are generally greater than the measurements by approximately 20 to 80 percent. Calculations for the 400 meter location show the greatest discrepancy. This is due to surface moisture conditions in the immediate vicinity. That location has been filled with gravel to produce a dry, firm surface to facilitate the handling of large shielding objects and, hence, creates fewer thermal neutrons per unit total fluence of neutrons incident on the ground.

Figure 2-3 shows the ratios of calculated to measured cadmium difference ratios. The cadmium difference ratio is that between the activated bare foil and the activated cd-covered foil and is therefore always greater than unity. The calculated values are generally within twenty percent of the measurements, indicating that, although the absolute fluence values may differ between calculation and measurement, the two are in good agreement as to the relationship between total and epithermal fluence in the gold cross section range.

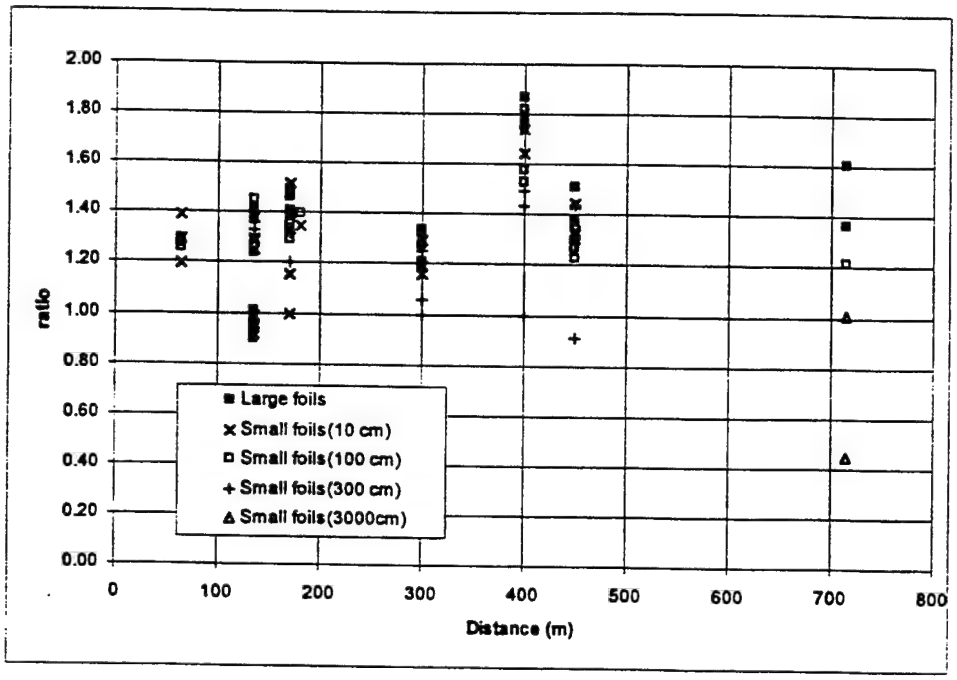

Figure 2-2. Gold foil activation (Cadmium difference) calculation to measurement ratio.

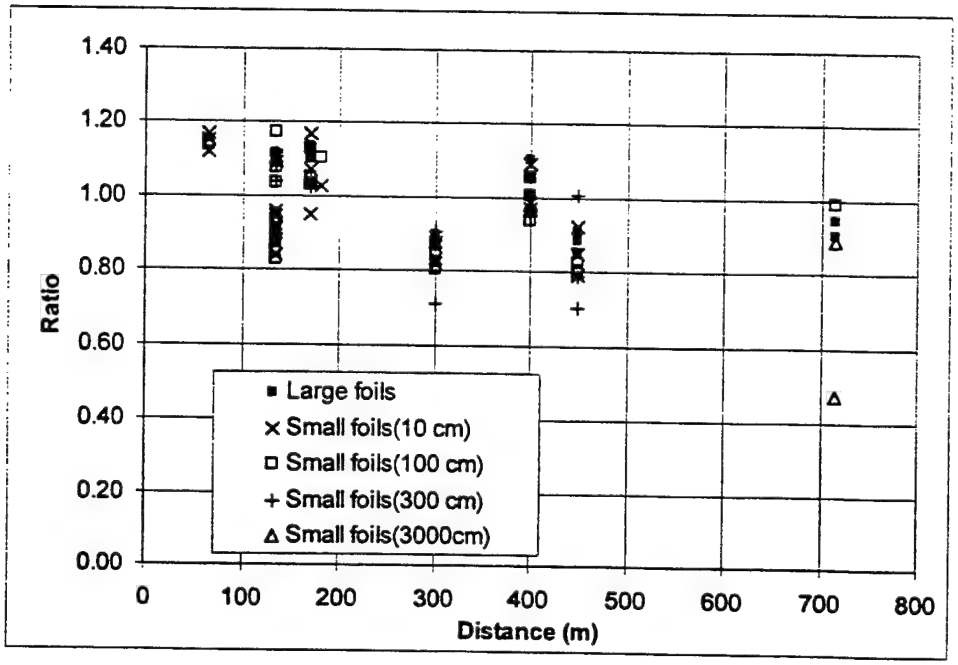

Figure 2-3. Gold foil activation cadmium ratio calculation to measurement ratio.

Figures 2-4 and 2-5 show the effect of height above the ground on thermal fluence as measured and calculated, respectively. The effect is depicted relative to the 100 cm measurement height. The measurements demonstrate a considerable amount of scatter. However, they generally show that the thermal fluence is greater at 10 cm and less at 300 cm. The calculations show the same effect and to approximately the same degree of magnitude.

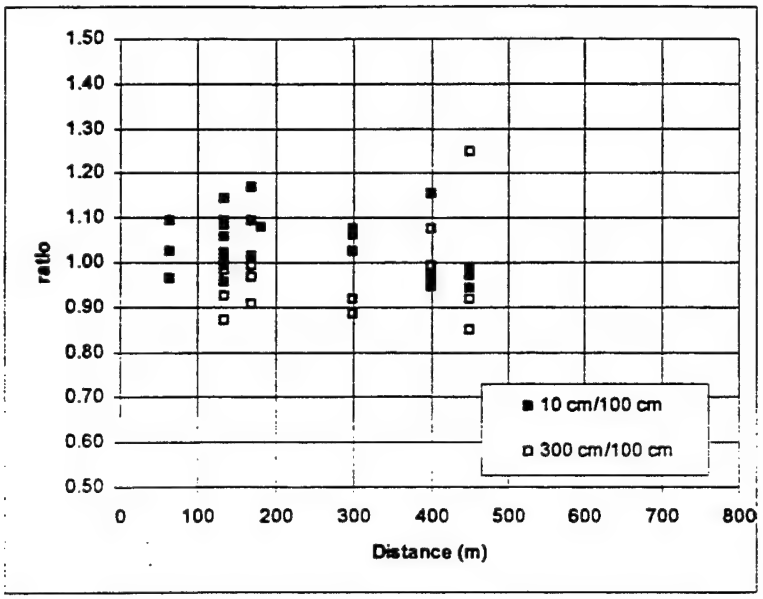

Figure 2-4. Thermal neutron height effect as measured by gold foils.

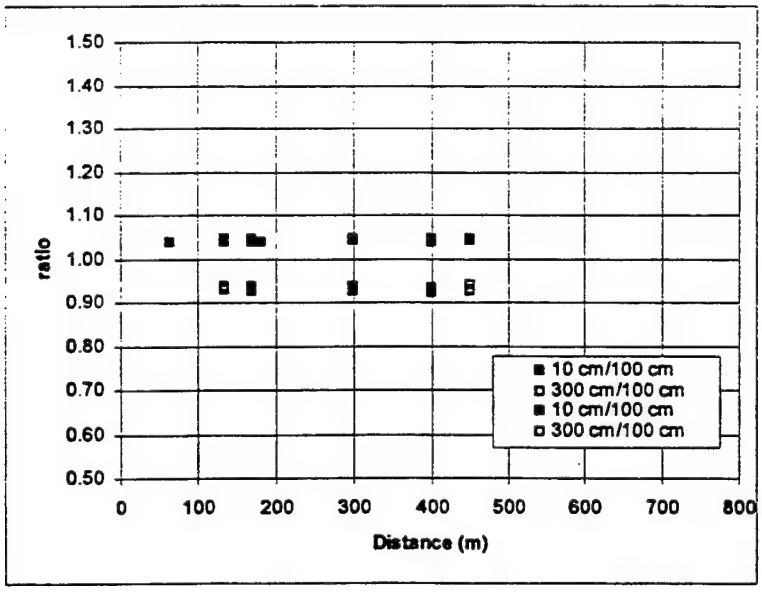

Figure 2-5. Thermal neutron height effect as calculated for gold foils.

2.2.2 Chlorine Transmutation (LLNL).

Accelerator mass spectroscopy is used to determine the number of Cl-35 nuclei transmuted to Cl-36. Cl-35 has a capture cross section that varies as a nearly perfect inverse of neutron speed (1/V) in the thermal and epithermal range, with no significant resonances. Thus, it is not necessary to use a cadmium cover to obtain good thermal neutron measurements using Cl-35. Calculations and measurement results are reported in terms of the effective 2200 meter/second fluence. Figure 2-6 shows the calculation to measurement ratio for Chlorine transmutation. The calculations are generally within twenty percent of the calculations, with no particular trend with distance. Note that, in the case of the gold measurements, the calculations at 400 meters were significantly out of range of the comparisons at other locations, this being caused by dry conditions resulting from gravel back fill at that location. In the case of the chlorine measurements, results were obtained during a very wet period in the Spring, when there was even standing water in the gravel. Hence, there is no recognizable anomalous behavior of measurement results at 400 meters in this case.

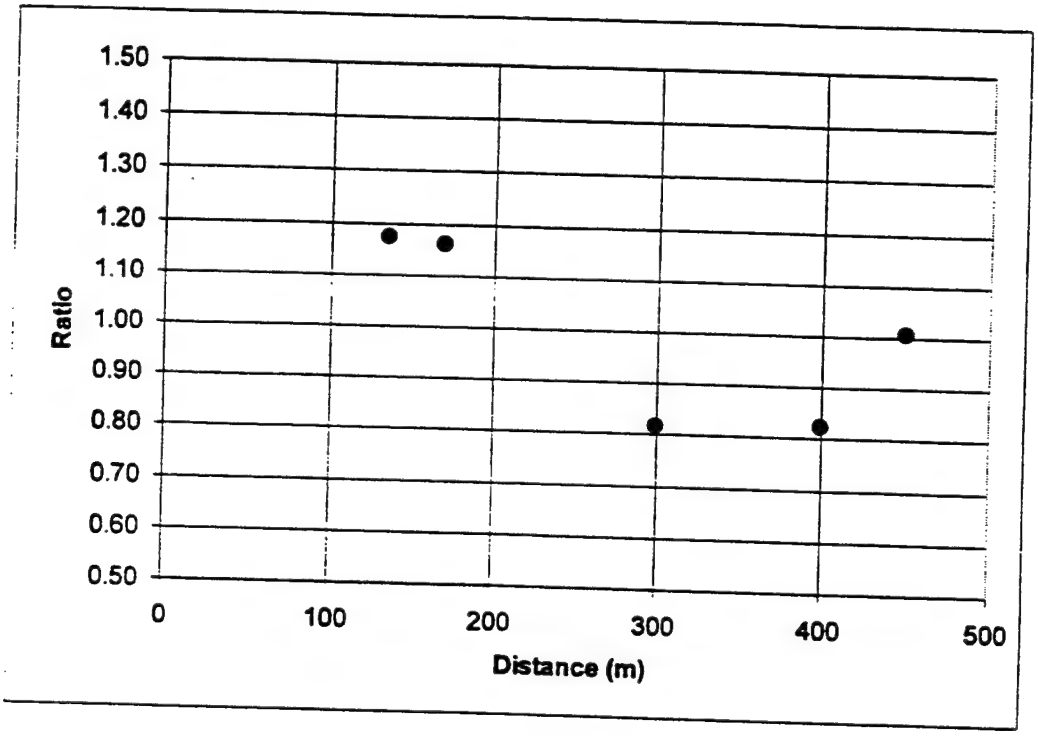

Figure 2-6. Chlorine foil transmutation, calculation to measurement ratio for thermal neutron fluence.

2.2.3 Bf3 Measurements (APRF).

The Bf3 proportional counter responds to low energy neutrons similarly to Cl-35, that is, as a nearly pure 1/V absorber. The response of a bare Bf3, as measured by Hajnal[2] is illustrated in Figure 2-7. In actual practice a pair of counters, one bare, the other cadmium covered, were deployed at each site. The difference between the two measurements is reported as the total Bf3 thermal fluence, referenced to the 2200 meters/second response.

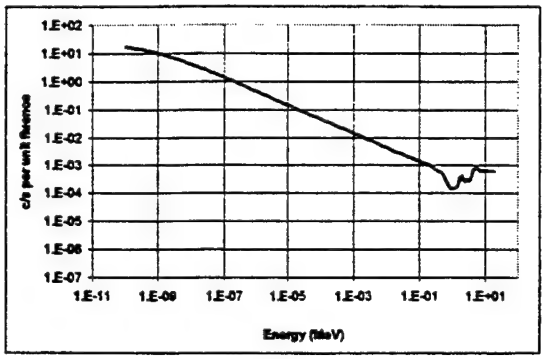

Figure 2-7. Bare Bf3 neutron response.

As shown in Figure 2-8, thermal fluence calculations are generally greater than those reported from the Bf3 measurements. This is particularly true at 400 meters and 715 meters. At these locations the assumptions of flat, uniform and unobstructed ground surface are probably inadequate to correctly model conditions under which the measurements occurred. The 400 meter location has surface characteristics that differ from other measurement sites, namely, that great care has been taken at that location to backfill an area of approximately 5 meters by 5 meters with gravel, thereby creating a very dry surface local to the measurements at that site. At 715 meters the measurements were performed along a right of way through trees, the nominal height of which was on the order of 30 meters. These trees shield the measurement location and are not accounted for in the calculations referred to here.

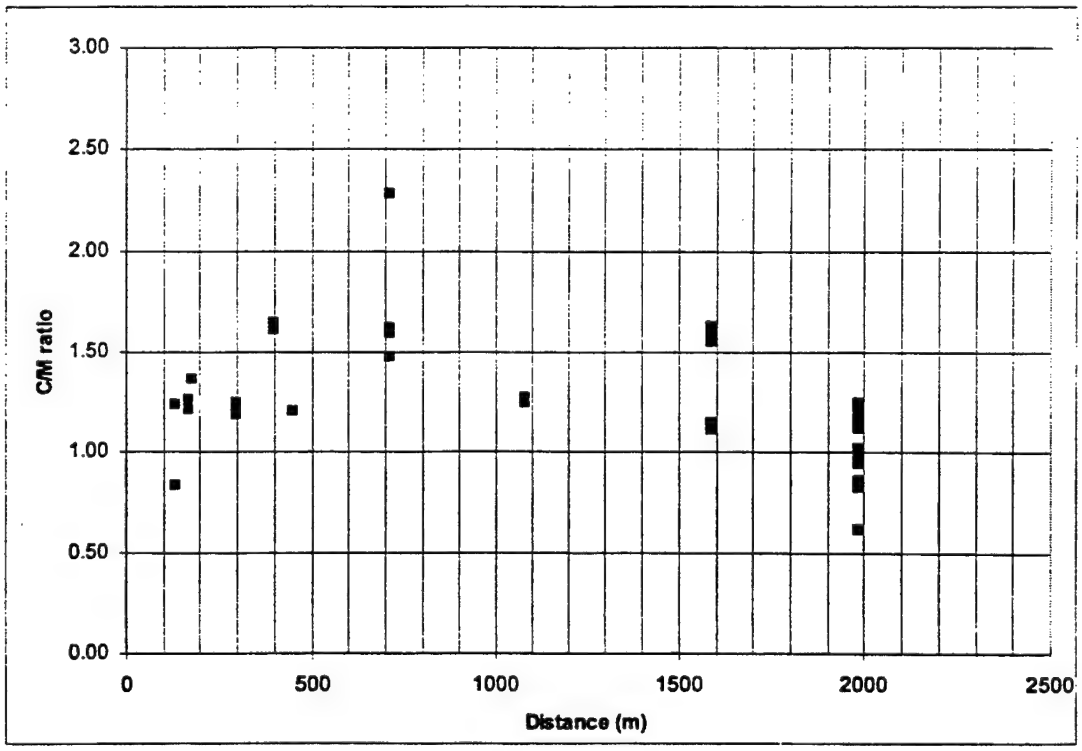

Figure 2-8. Bf3 (Cadmium difference) calculation to measurement ratio.

2.2.4 Sulfur Activation (APRF).

Sulfur activation measurements were performed to a distance of 715 meters. The results of these measurements are reported in terms of neutron fluence having energies greater than 3 MeV. Figure 2-9 shows the calculation to measurement ratio for the sulfur activation results. At distances beyond approximately 400 meters the measurements are scattered over a wide range of values, including some negative net values. Nevertheless, the agreement between the calculations and measurement is generally very good.

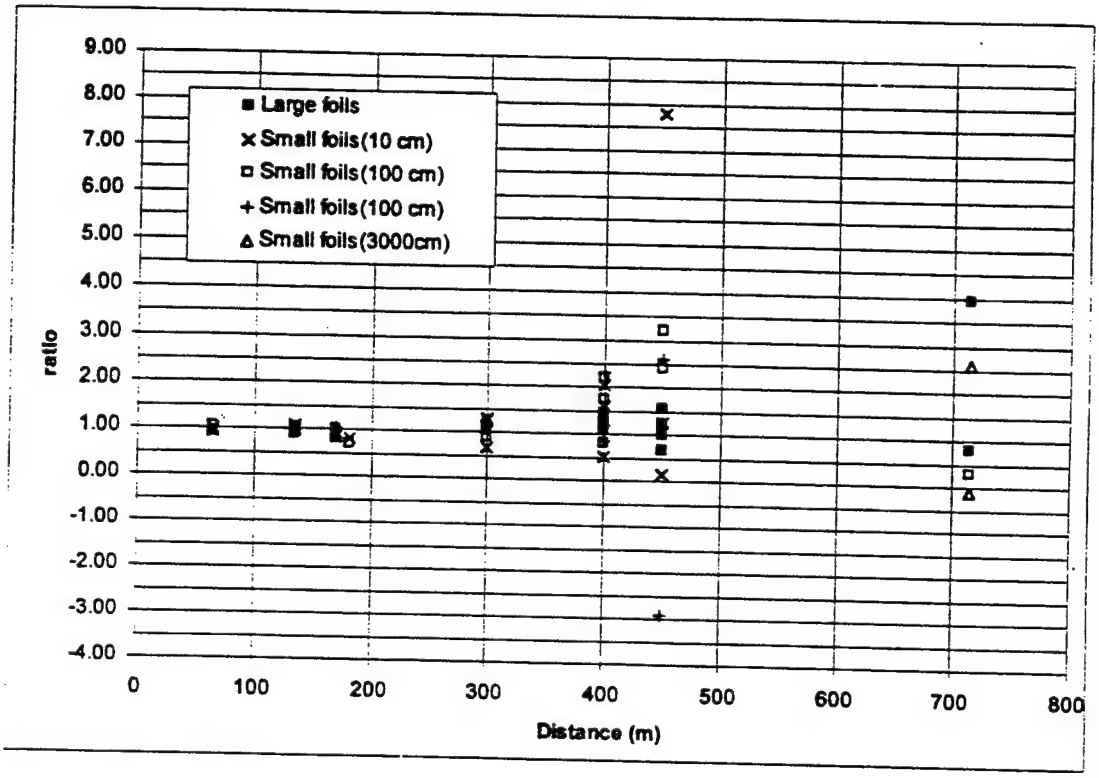

Figure 2-9. Sulfur activation calculation to measurement ratio.

2.2.5 Remmeter Measurements (APRF).

A remmeter consists of a cadmium covered Bf3 proportional counter, deployed inside of a polyethylene sphere. The remmeter was calibrated in bare and D_20 shielded Cf-252 fields and interpolated to obtain a response consistent with the neutron spectrum expected at 400 meters. The results of the remmeter measurements were reported in terms of absorbed (tissue) dose (mrad/kwhr) and dose equivalent (mrem/kwhr).

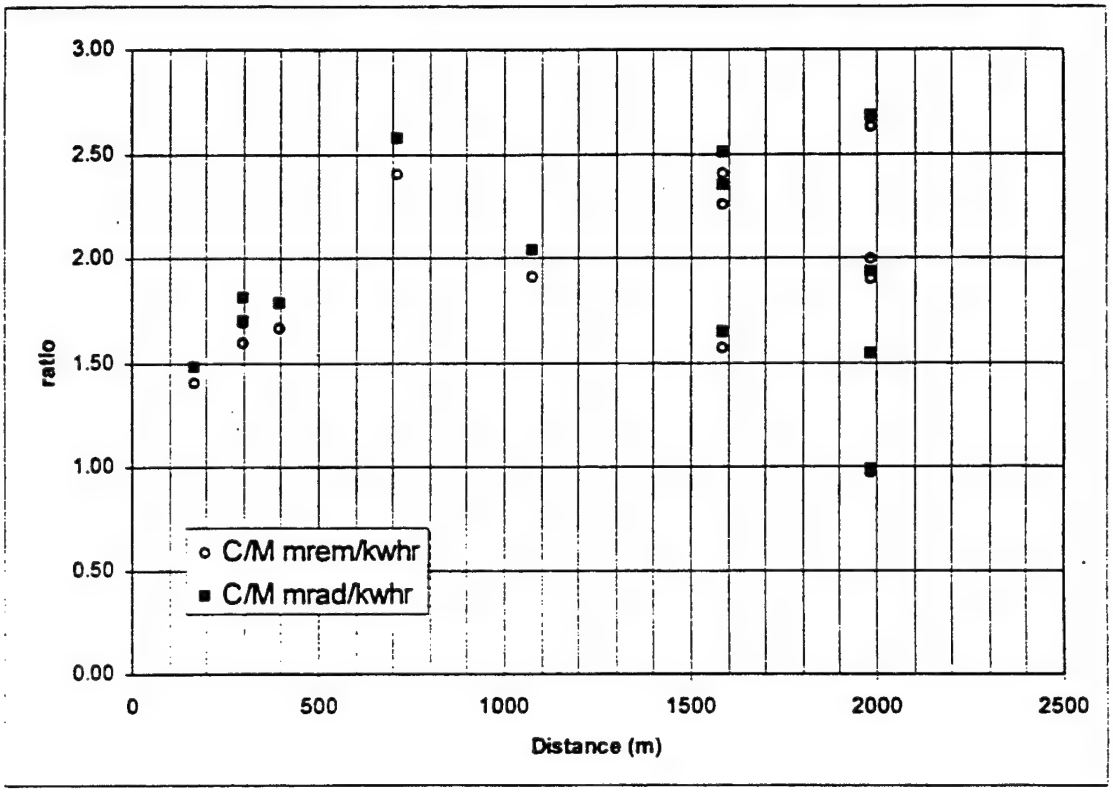

Figure 2-10. Neutron doses & dose equivalents as measured by remmeter, calculation to measurement ratio .

Figure 2-10 shows the comparison between calculated and measured neutron dose and dose equivalent. The calculations are generally on the order of fifty percent greater than the measurements, with the discrepancy being in the same direction but much larger at some locations. The 300 meter and 400 meter sites are partially shielded by trees, though not in the line of sight from the reactor. The 715 meter site is shielded in the line of sight to the reactor by a similar growth of trees. The effect of the trees is addressed later in this report.

2.2.6 Proton Recoil (ROSPEC) Measurements (APRF, DREO).

The ROSPEC neutron spectrometer measures fluence spectra in the energy range from approximately 50 keV to 4 MeV. Two laboratories fielded the ROSPEC, Army Pulsed Radiation Facility and Defence Research Establishment Ottawa. As shown in Figure 2-11, the calculations are greater than the APRF measurements at all locations, with some differences exceeding sixty percent. The calculations are generally within plus or minus twenty percent of the DREO measurements, though in some cases the calculations exceed the measurements by approximately forty percent. There also appears to be a slight trend in the comparison, with the calculation to measurement ratio rising with increasing distance.

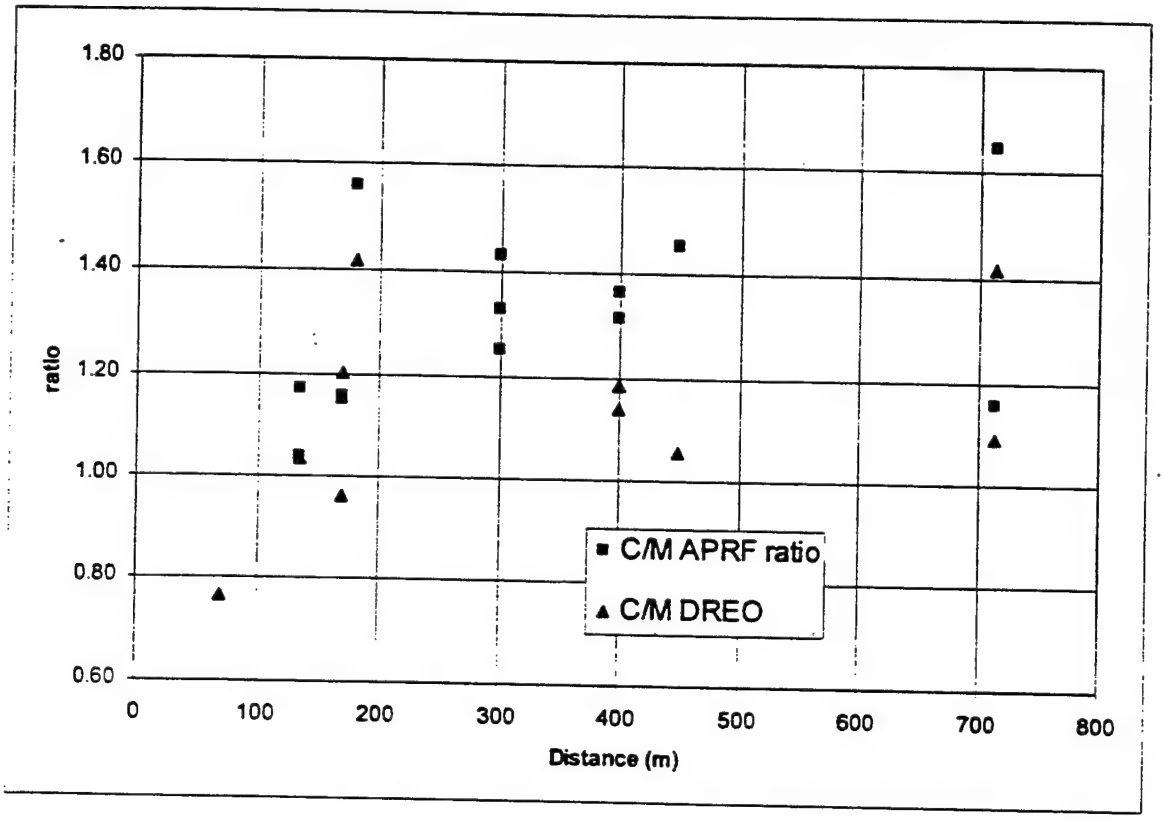

Figure 2-11. Proton Recoil (ROSPEC) neutron doses calculation to measurement ratio.

2.2.7 Boron-Loaded plastic Scintillator (LANL).

Los Alamos National Laboratory fielded a very sensitive neutron spectrometer at two locations at APRF, 1080 meters and 1620 meters. The LANL spectrometer measured neutron fluence spectra in the energy range from approximately 400 keV to approximately 20 MeV. As shown in Figure 2-12, the measured fluence was converted to dose and compared with calculated dose in the same energy range. Comparisons were also made between calculated and measured fluences above 3 MeV. The calculated neutron dose exceeds the measurements by on the order of sixty percent, while the calculated neutron fluence, equivalent to that which would be measured by sulfur, exceeds the measurements by between ten and forty percent. The fluence comparison appears to worsen with increasing distance.

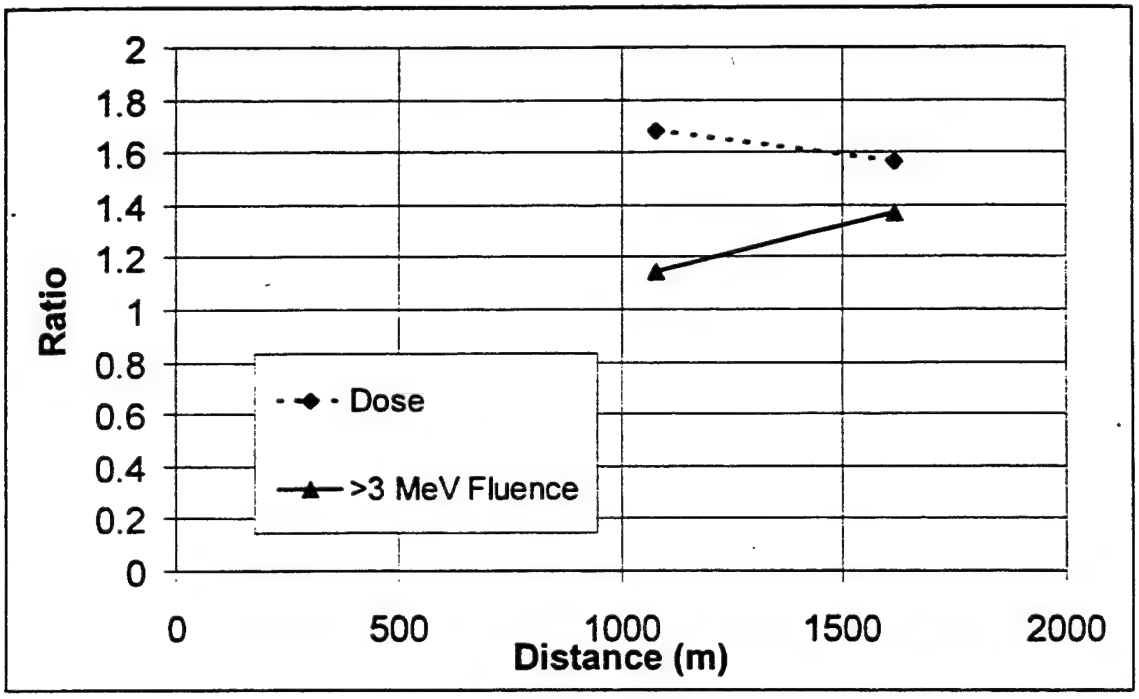

Figure 2-12. Boron-Loaded Plastic Scintillator dose and fluence (>3 MeV) calculation to measurement ratios.

2.2.8 Bonner Ball Measurements (EML).

Bonner Balls (or Bonner Spheres) are a collection of cadmium covered, polyethylene shrouded Bf3 proportional counters. Each shroud has a different diameter, thereby thermalizing and rendering detectable by the Bf3 a different energy range of incident neutron spectra. The resulting array of measured values are unfolded, using an iterative technique and an estimated initial spectrum guess. The spectral regime controlled by each Bonner Ball is relatively broad, on the order of ten to twenty percent of the energy value. Therefore, if the initial guess has an energy resolution that is better than this, the fine detail of the initial estimate is preserved. The unfolding process cannot add create such detail.

Figure 2-13 shows ratio of calculated to measured tissue dose (free in air) values. Calculated and measured spectra were both weighted with tissue kerma to obtain these values. Aside from the one anomalous point at 715 meters, the comparison between calculation and measurement is quite consistent. The calculated values are twenty to forty percent greater than the measurement. Further, there appears to be a trend toward greater discrepancy with increasing distance. The two values at 715 meters are actually for the same reported measurement. In the case of the lower ratio value, the surrounding trees have been accounted for, whereas in the case of the upper ratio value they have not. The effect of the trees is discussed further in a later section of this report.

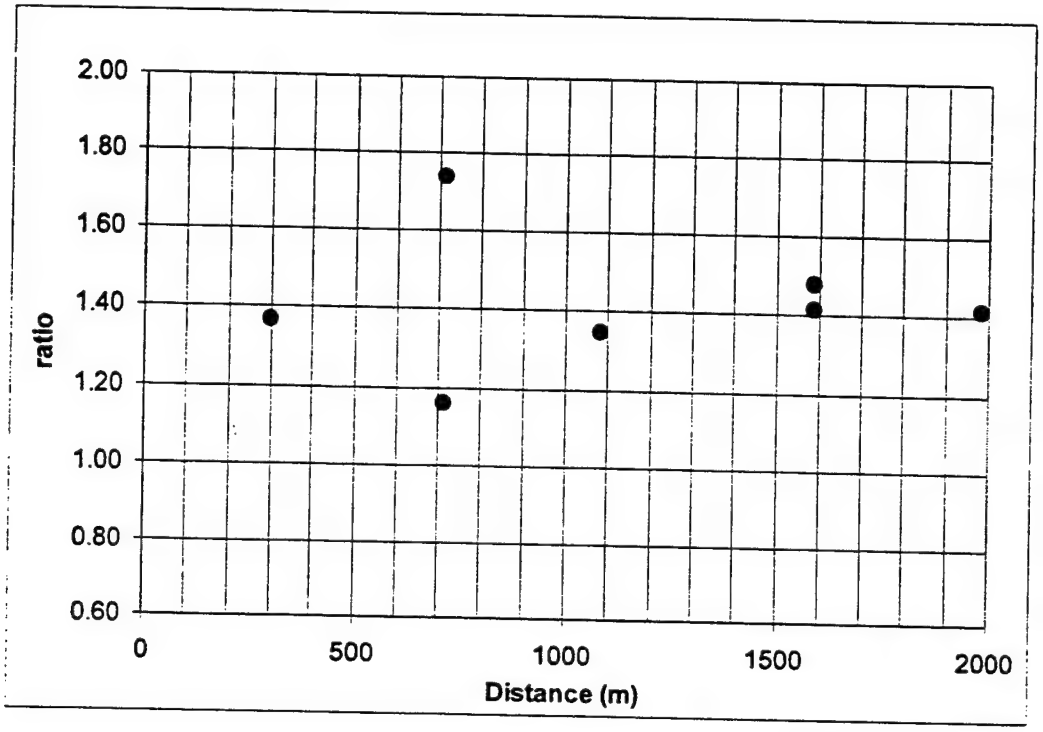

Figure 2-13. Bonner Ball neutron dose calculation to measurement ratio.

Figure 2-14 shows the calculation to measurement ratio for neutron fluence having energies greater than 3 MeV. As in the case of the neutron dose, aside from the one anomalous point at 715 meters, the comparison between calculation and measurement is quite consistent. The calculated values are twenty to forty percent greater than the measurement. Further, the a trend toward greater discrepancy with increasing distance appears to be more pronounced than in the case of the dose. The two values at 715 meters are actually for the same reported measurement. In the case of the lower ratio value, the surrounding trees have been accounted for, whereas in the case of the upper ratio value they have not. The effect of the trees is discussed further in a later section of this report.

Figure 2-15 shows the calculation to measurement ratio for neutron spectra at distances from 300 meters to 2000 meters. The comparison at 715 meters shows the calculations anomalously high due to the absence of surrounding trees in the calculation. Below 1 MeV the calculations are approximately forty percent larger than the measurements. Above 1 MeV the comparison reflects the data shown previously, that the discrepancy increases from approximately twenty percent to over forty percent, with increasing distance.

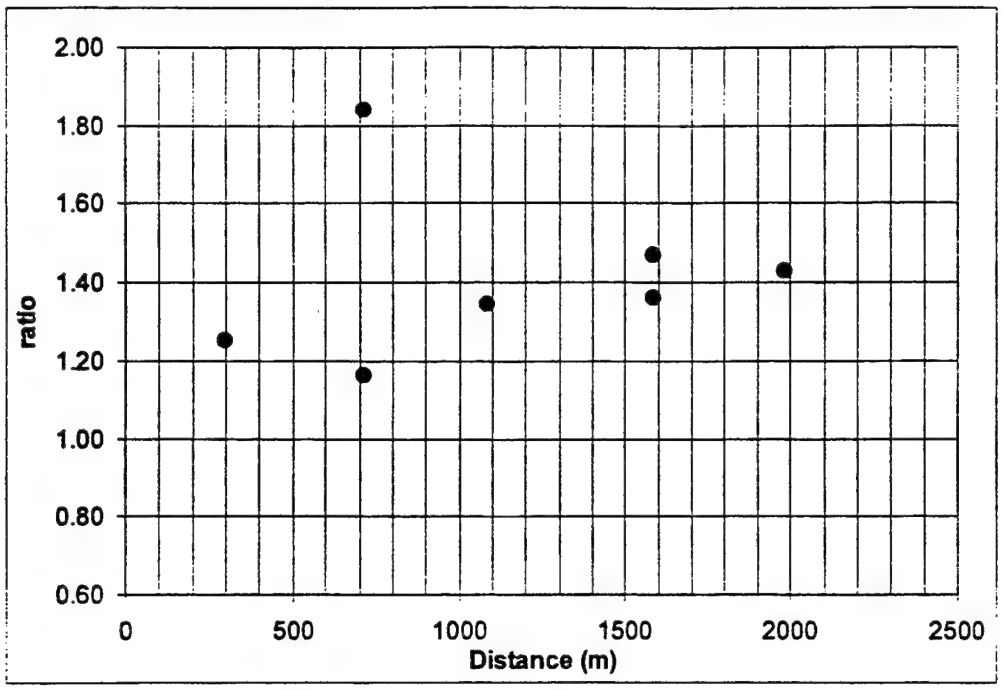

Figure 2-14. Bonner Ball greater than 3 MeV neutron fluence calculation to measurement ratio.

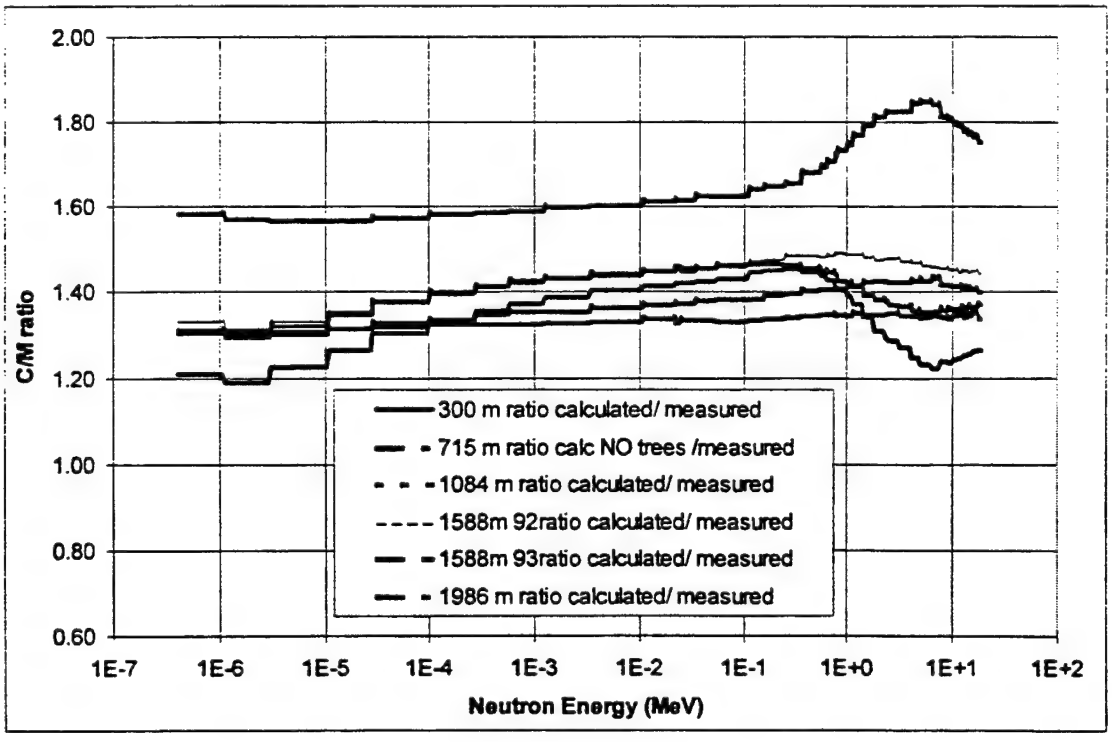

Figure 2-15. Bonner Ball neutron fluence spectra calculation to measurement ratio.

2.2.9 Thermoluminescent Dosimetry (APRF).

Thermoluminescent (TLD) gamma ray dose measurements were performed with three different types of dosimeters, CaF_2, LiF and Al_2O_3. All but the LiF were deployed with thin aluminum covers to prevent effects of light exposure from interfering with the measurements. The LiF dosimeter was shielded with additional lithium to reduce the influence of thermal neutrons. The CaF_2 was also deployed with a thin tin cover to reduce sensitivity to low energy photons. The effect of the shields were accounted for in the calculations by using perturbed fluence to dose conversion factors.

Figure 2-16 shows the calculation to measurement ratios for CaF_2 , small and large foils, at distances from 75 meters to 715 meters. Except for the large variability of measured results at 135 meters, primarily involving small foils, the results are reasonably consistent, with calculations varying plus and minus approximately twenty-five percent from the measurements. There also appears to be a tendency for the calculations to increase with respect to the measurement with increasing distance. Finally, the calculations do not account for the presence of terrain or foliage variations at the measurement sites. This has already been shown to be important to the neutron comparisons, particularly at 400 meters and at 715 meters. The comparison of calculated and measured gamma ray dose does not reveal a similar importance for gamma rays.

CaF_2 dosimeters were deployed at three heights above the ground. No consistent trend to calculation to measurement comparisons having to do with detector height is apparent.

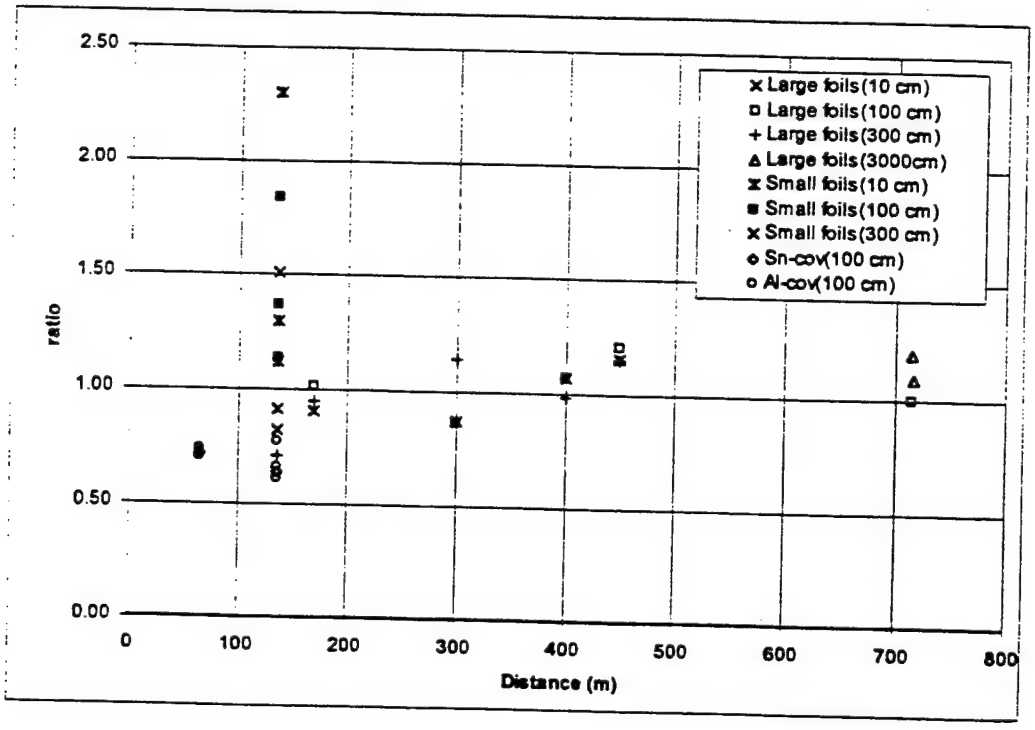

Figure 2-16. CaF2 TLD gamma ray dose calculation to measurement ratio.

Figures 2-17 and 2-18 show the calculation to measurement ratios for the LiF and Al_2O_3 measurements. In each case the comparisons lie in a range of forty percent. In the case of LiF this range is centered on unity, while in the case of Al_2O_3 the range is centered on eighty percent. There is considerably less variability at the 135 meter distance than was the case the for CaF_2. Also, once again, no strong trend in the ratios can be seen as a result of detector height above the ground.

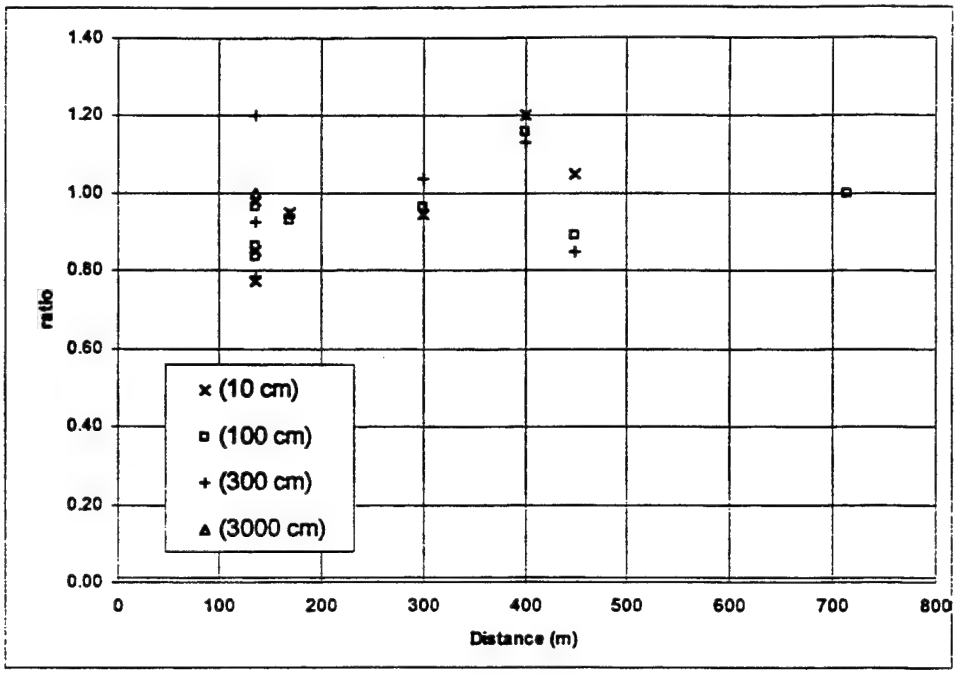

Figure 2-17. LiF TLD gamma ray dose calculation to measurement ratio.

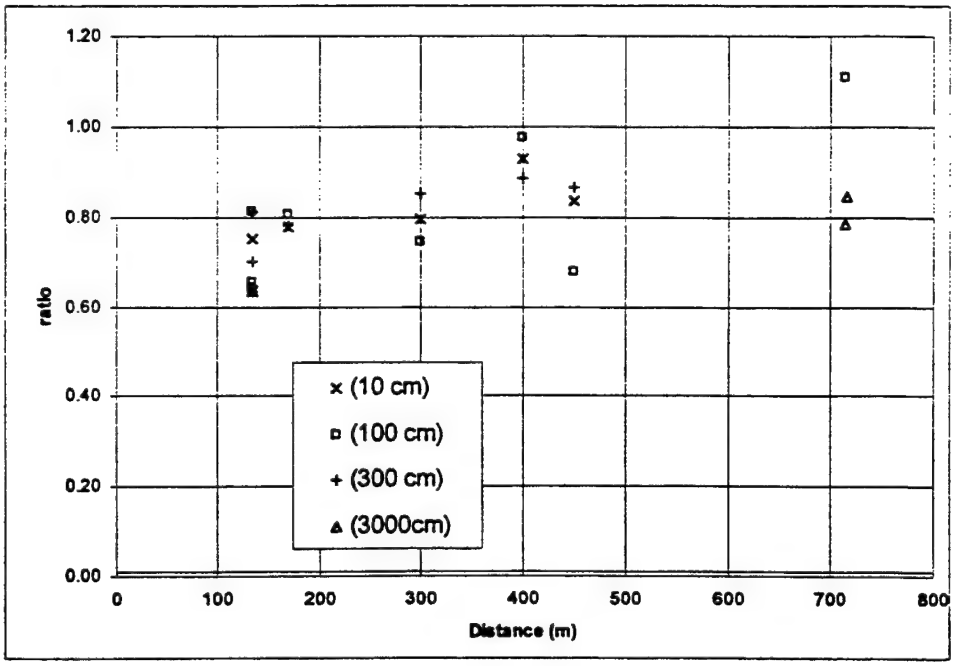

Figure 2-18. Al_2O_3 TLD gamma ray dose calculation to measurement ratio.

2.2.10 Geiger Counter Gamma Ray Measurements (APRF).

A Geiger Counter is the equivalent of a remmeter, in that it must be calibrated for a specific spectrum and is only valid for that spectrum. Fortunately, in the case of gamma rays the spectrum is more stable with increasing distance from the source and in the presence of other perturbing factors, such as forest and terrain, than is the case for neutrons. Thus, the agreement between calculations and measurements shown in Figure 2-19 is excellent, at least until the signal becomes so low at 2000 meters that the measurement variability becomes vary large.

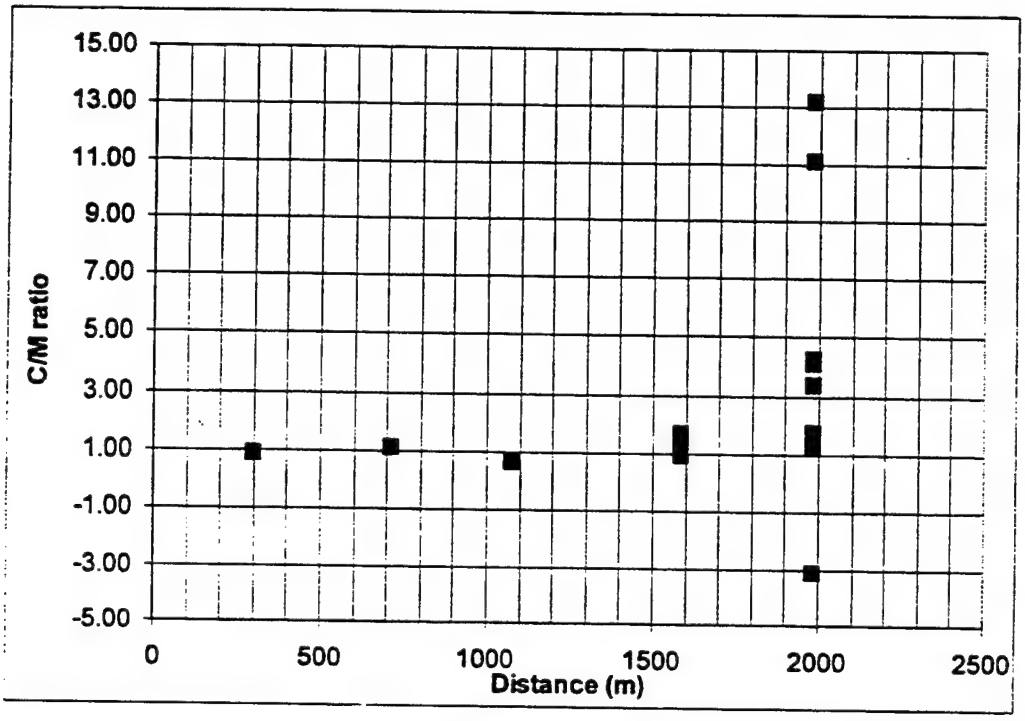

Figure 2-19. Geiger Counter, gamma ray dose calculation to measurement ratio.

As noted previously, the calculations do not take into account the presence of non-uniform terrain or the effects of local shielding by forest. Nevertheless, the agreement with measurement is very good, even at the 400 meter and 715 meter locations, where differences between calculated and measured neutron dose was so pronounced.

SECTION 3
MODIFICATIONS TO CALCULATIONS

Section 2 of this report provides the results of comparisons between measurements and the basic MASH calculation. That calculation includes the APRF reactor leakage released by SAIC in 1990, ENDF/B-5 cross sections and flat terrain with no foliage. After those calculations were performed, three changes and additions to the initial conditions of the MASH calculation were considered. Modifications include accounting for the presence of non-uniform terrain and forest at the APRF site and the addition of ENDF/B-6 cross sections. This section of the report provides the results of those modifications.

3.1 EFFECTS OF CALCULATION MODIFICATIONS AT 170 AND 400 METERS.

The effect of the inclusion of ENDF/B-VI cross sections, non-uniform terrain and foliage on calculated fluence has been investigated at 170 and 400 meters for neutrons and gamma rays. The terrain effect was investigated using the DORT, 2-dimensional discrete ordinates module of MASH, while the foliage effects were assessed using the MORSE, 3-dimensional Monte Carlo module.

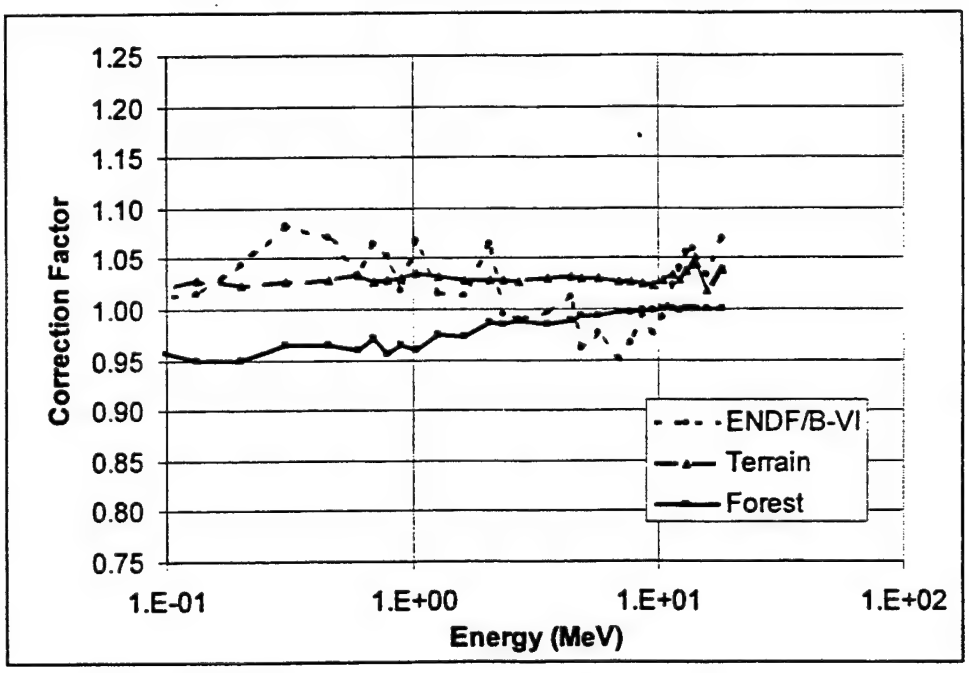

Figure 3-1. Factors for correcting MASH calculated neutron fluence at 170 m for ENDF/B-6 cross sections, non-uniform terrain and forest.

According the Figures 3-1 and 3-2, the effect of the terrain is small on neutrons in the energy range important to kerma, 100 keV < En < 20 MeV, causing an increase on the order of 3% at 170 and having virtually no effect at 400 meters. The effect of terrain is more pronounced for thermal fluence (not shown in the figure), increasing the value at 170 meters by approximately 12% and at 400 meters by approximately 7%. In between the highest and lowest energy regions the terrain causes a depletion of fluence, particularly in the range of 1 to 10 eV.

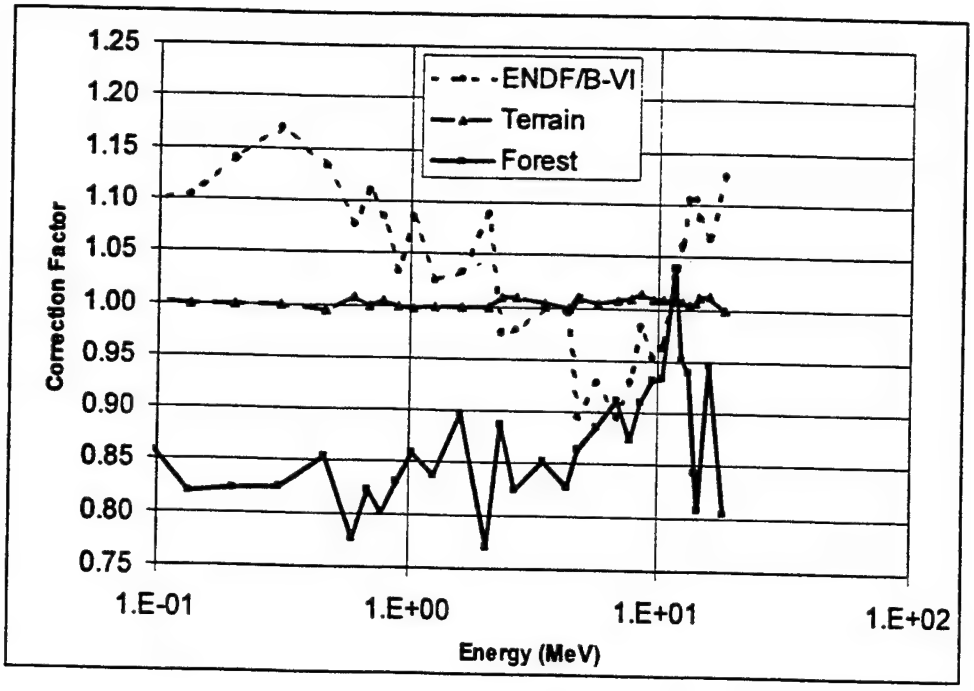

Figure 3-2. Factors for correcting MASH calculated neutron fluence at 400 m for ENDF/B-6 cross sections, non-uniform terrain and forest.

The propagation of neutrons above 10 MeV is enhanced through the use of the new cross sections. However, this has no importance for the APRF application. As might be expected, the effect of the cross sections is larger for the larger amount of material traversed, which corresponds to the 400 meter distance.

The effect of including the forest is to substantially reduce the neutron fluence between 100 keV and 10 MeV. This is approximately the inverse of the effect of switching to ENDF/B-VI cross sections. However, the kerma perturbation caused by the forest is dominant because it most effects neutrons having energies between 500 keV and 4 MeV.

Effects of cross sections, terrain and foliage on Gamma Ray Fluence have not been completely determined. ENDF/B-VI cross sections for secondary gamma ray production were not available at the time calculations were made for the measurement corridor out to 400 meters. However, as shown in Figures 3-3 and 3-4, the effect of both the terrain and forest is to increase the gamma ray fluence, a logical consequence of the increase in thermal neutron fluence shown previously. The effect is largest at 170 meters, since the neutron fluence is larger there, relative to the gamma rays, than it is at 400 meters. At 170 meters the terrain causes an increase in the gamma rays from materials in the ground, hydrogen, aluminum, silicon and iron, but has little effect on gamma rays typically associated with neutron capture in the air, such as the 5.5 MeV and 11 MeV nitrogen gamma rays.

The forest also results in an increase in gamma rays at 170 meters, with peaks at 2.3 MeV, hydrogen capture, and 5.5 MeV and 11 MeV, nitrogen capture. A large increase in very low energy photon fluence (not shown) is thought to be caused by a statistical aberration, probably related to under-sampling of particles in this group. The statistical precision in that group as expressed as a coefficient of variation is 32%, compared to 3% or better for all other groups. In any event the contribution to kerma at this energy is negligible.

At 400 meters the terrain causes a small enhancement, on the order of a couple of percent, of the high energy gamma rays. The forest causes a large increase in the gamma ray lines from hydrogen and nitrogen. However, the dominant effect of the forest is to shield the 400 meter location from scattered gamma rays.

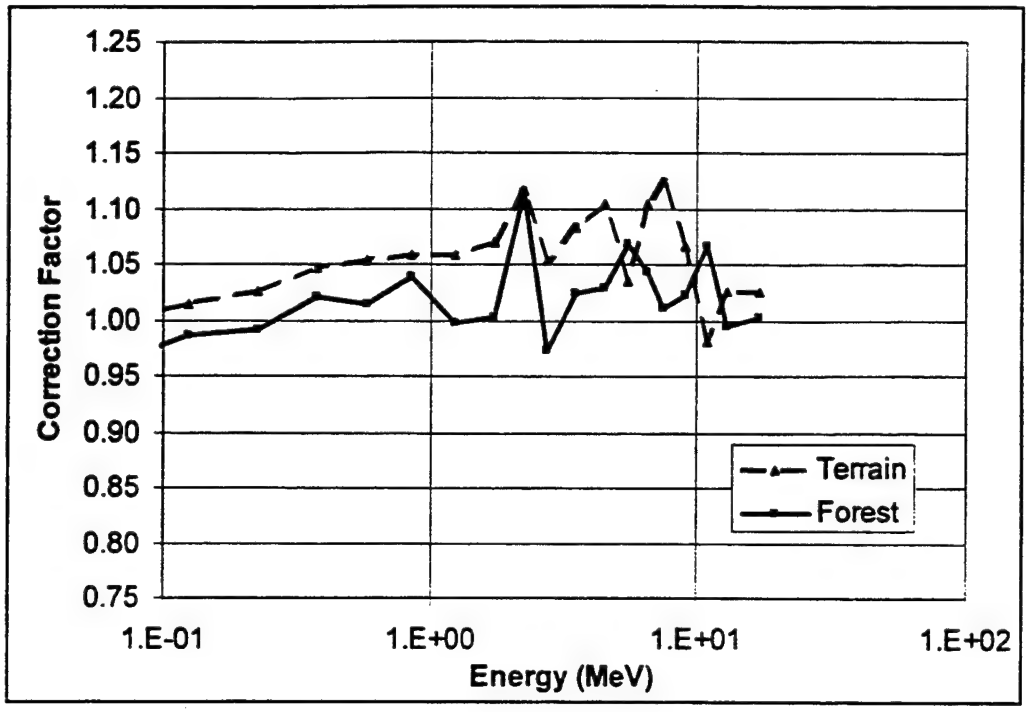

Figure 3-3. Factors for correcting MASH calculated gamma ray fluence at 170 m for non-uniform terrain and forest.

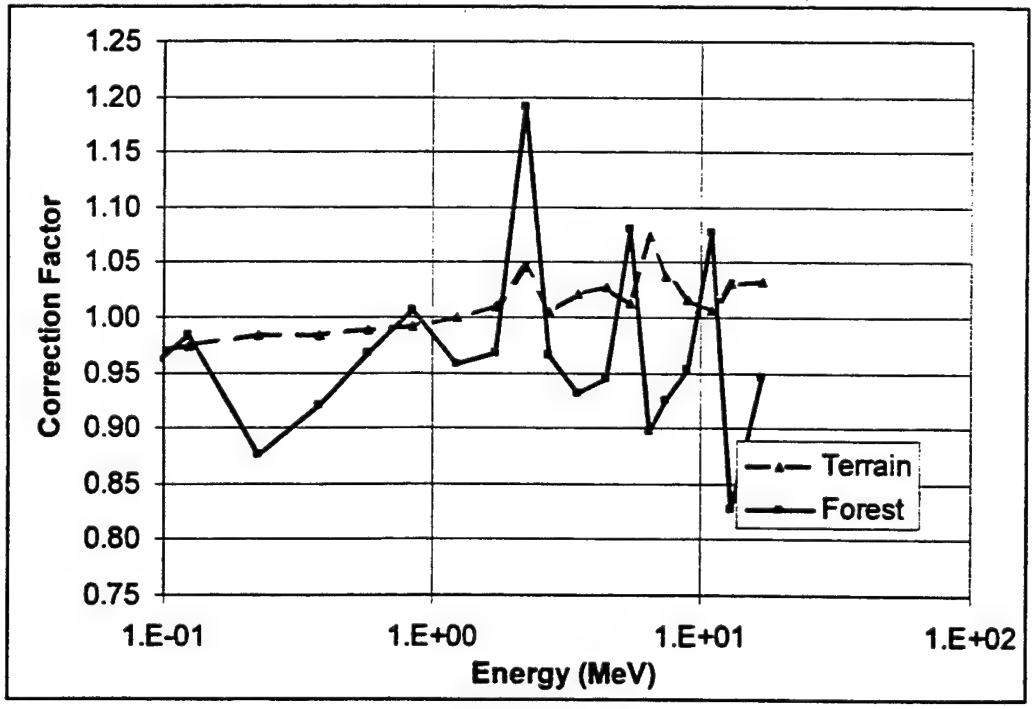

Figure 3-4. Factors for correcting MASH calculated gamma ray fluence at 400 m for non-uniform terrain and forest.

3.2 THE EFFECT OF THE FOREST AT 715 METERS.

In order to compare to some of the measured values, local perturbations to shielding conditions around the detector must be accounted for. For example, the road at 715 meters from the reactor is surrounded by trees on both sides. Earlier studies have shown that a nearby forest of trees perturb the neutron fluence significantly, by shielding higher energy particles, thus reducing dose, and by allowing scatter close to the detector, thus increasing the lower energy scattered components of the neutron fluence. The road clearing is at a 45 degree to the reactor line of sight and cannot be modeled in two-dimension R-Z geometry.

The MORSE Monte Carlo component of the MASH code is used to calculate the radiation fluence, perturbed by local shielding, which differs from that obtained from the DORT R-Z geometry. MASH calculates the local radiation fluences by using the adjoint Monte Carlo method to transport radiation response as a source importance from the detector location out of the shield to produce an adjoint fluence. A companion code, DRC, then is used to fold together the adjoint fluence with the free-field fluences calculated by DORT. This allows one to calculate the fluence and responses at the detector location in local shielding exposed to the free field fluences at APR.

The local shielding is first modeled by combining solid geometry ("primitive") objects. The model of the road in the forest consists of a 100m x 100m x 16m box, containing the average mixture of tree and air in a forest. A 100m x 100m x 1m box of ground is placed below the tree/air region. The road clearing in the forest is obtained by placing a box of air 100m x 9.8m x 16m through the center of the tree/air region. The 9.8m is the width of the road shown on maps of the area around APR. The clearing may be wider at some places along the road. Pictures taken at the time of the measurements show that near some of the measurements the distance from the edge of the road to the closest trees is approximately the same width as the road. Therefore, a second model of the clearing using a 100m x 30m x 16m box of air is included to examine the effect of the width of the clearing. The detector is located 125 cm above the ground, in the center of the road and at 2.5m from the edge of the road. It is also placed 30m above the center of the road. For the tree problem 750,000 particle histories were started. These numbers are adequate to calculate the dose and spectra to a statistical uncertainty less than 1% and 5%, respectively.

The neutron and gamma-ray cross sections used in the calculation of forest-shielding effects are from the DABL69 library (ENDF/B-V) and are part of the MASH system. The material constituents consist of air, air-tree mixture, and ground for the "road in the trees" problem. The elemental densities are given for both the materials in the free-field DORT calculation and the local-shield MASH calculation in Table 3-1.

Table 3-1. Elemental constituents used in forest perturbation calculations.

	Elemental Densities (atoms per barn-centimeter)							
	Air			Ground				Air/Tree
Run	240	241	66	240/241		66		
				10%h2o > 500 m	25%h2o < 500 m	33%h2o > 500 m	50%h2o < 500 m	
H	7.35-7	9.36-7	1.33-7	9.88-3	2.47-2	3.26-2	4.94-2	1.02-4
C				1.66-3	1.66-3	1.66-3	1.66-3	7.05-5
N	3.78-5	3.81-5	4.08-5	5.19-5	5.19-5	5.19-5	5.19-5	2.41-7
O	1.09-5	1.11-5	1.15-5	3.28-2	4.02-2	4.42-2	5.26-2	4.57-5
Na				1.57-4	1.57-4	1.57-4	1.57-4	
Mg				1.00-4	1.00-4	1.00-4	1.00-4	
Al				1.51-3	1.51-3	1.51-3	1.51-3	
Si				1.06-2	1.06-2	1.06-2	1.06-2	
P								1.08-7
S				3.83-6	3.83-6	3.83-6	3.83-6	
Cl				3.76-6	3.76-6	3.76-6	3.76-6	
Ar	2.26-7	2.28-7	2.44-7					
K				2.25-4	2.25-4	2.25-4	2.25-4	
Ca				1.28-3	1.28-3	1.28-3	1.28-3	
Mn				8.01-6	8.01-6	8.01-6	8.01-6	
Fe				3.52-4	3.52-4	3.52-4	3.52-4	
Cu				5.32-7	5.32-7	5.32-7	5.32-7	

Figure 3-5 shows the correction to the neutron fluence at the 715 meter measurement site due to the surrounding forest. Note that this correction does not include the effect of terrain, which was not calculated, or the inclusion of ENDF/B-VI cross sections, which was applied separately. The effects of the correction are to enhance the thermal neutron fluence, due to scatter in the hydrogenous, forested area, and to reduce the remainder of the fluence. The latter effect becomes more pronounced with increasing neutron energy. As can be seen from the figure, getting an accurate geometry portrayal of the area surrounding the measurement site is extremely important. Based on photos of the region the 30 meter-wide geometry was chosen as representative and the associated results used in subsequent corrections to the 715 meter fluence. Use of the 30 meter-wide clearing resulted in correction factors of approximately 66% for neutron dose, 122% for thermal neutron fluence and 61% for fast (>3 MeV) neutron fluence.

Figure 3-6 shows the correction factor for gamma ray fluence due to the presence of the forested area about the 715 meter site. The scattered fluence reaching the site is reduced by the forest mass. However, neutron capture in the forest hydrogen produces the spike at 2.2 MeV, which makes up for the deficit. The result is that the gamma ray dose correction factor is approximately 97%.

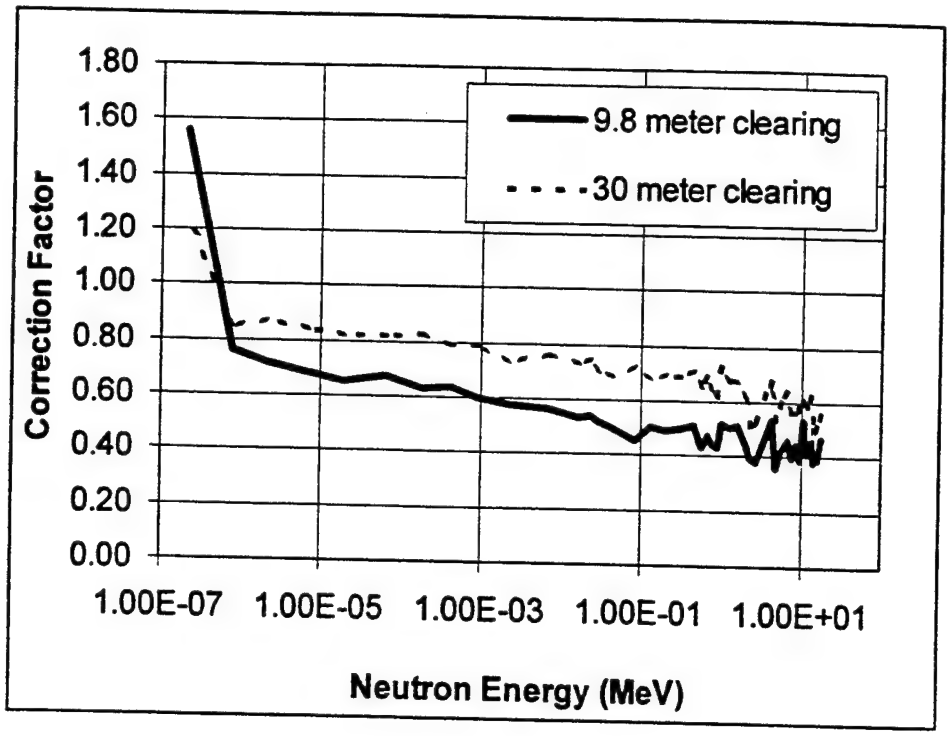

Figure 3-5. **715 meter measurement site, neutron fluence corrections due to surrounding forest.**

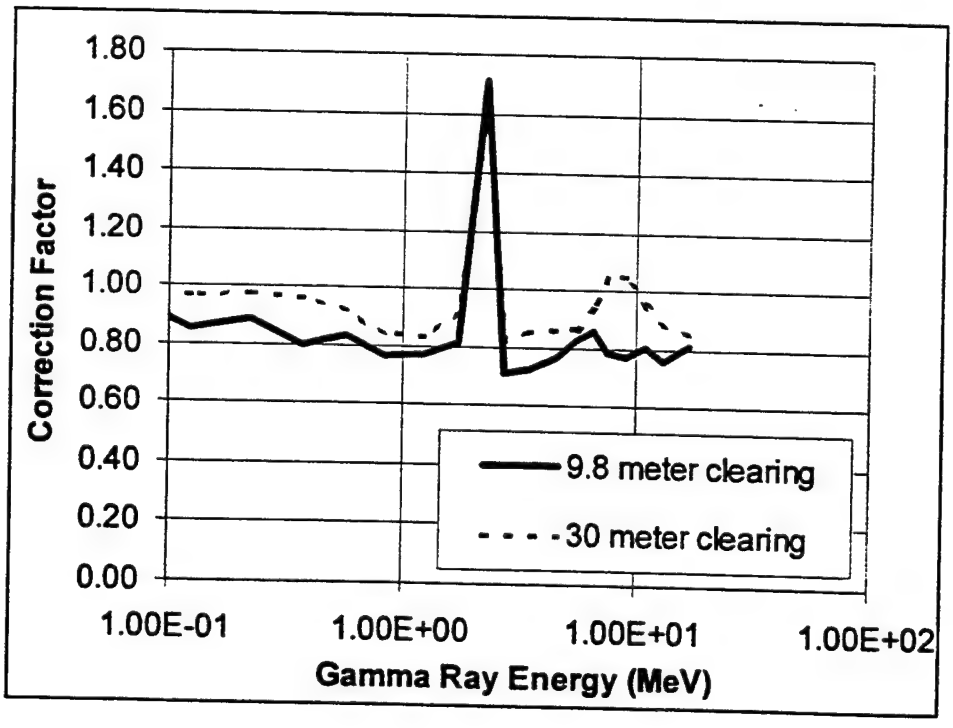

Figure 3-6. **715 meter measurement site, gamma ray fluence corrections due to surrounding forest.**

3.3 CORRECTED CALCULATION COMPARISON WITH MEASUREMENTS.

Corrections resulting from the use of ENDF/B-VI cross sections, the inclusion of terrain (at distances of 400 meters or less) and accounting for the presence of forest caused little change calculation to measurement comparisons for either the thermal neutrons or gamma rays. In fact, the inclusion of the terrain and forest corrections actually served to increase the thermal neutron fluence somewhat, resulting in a slight worsening of the comparison.

The effect of calculation corrections on neutron dose and high energy fluence was another matter, however. Figures 3-7 through 3-12 show calculation to measurement ratios before and after correction for sulfur activation, remmeter, ROSPEC, Bonner Ball and boron-loaded plastic scintillator. In each case the correction noticeably improved the calculation to measurement ratio.

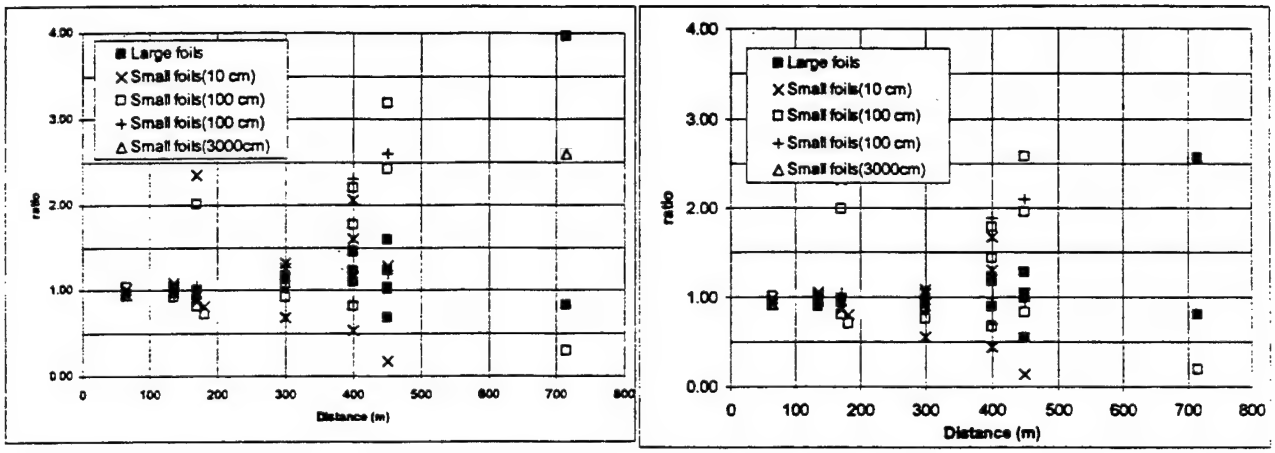

Figure 3-7. Sulfur activation calculation to measurement ratio, as calculated (left) and corrected (right).

Figure 3-7 shows the calculation to measurement ratios for the sulfur measurements. Note that in the corrected case at 715 meters both the large foil exposed ground level and the small foil exposed at 30 meters height lie on top of each other. Thus, the correction substantially improved the comparison on the ground, but gained little in the case of the elevated measurement. This theme is repeated in the case of ROSPEC measurements and may signify a conceptual problem in how to correctly model the elevated case.

Figure 3-8 shows the remmeter calculation to measurement ratios, uncorrected and corrected. Even with the large amount of scatter in the measurements the improvement obtained by the corrections is quite remarkable. Of course even with the corrections the calculations are greater than the measurements by approximately fifty percent. However, even this is of interest, because this consistent difference is similar to that seen in the case of the Bonner Ball results and to some extent the ROSPEC results, which were obtained by different laboratories.

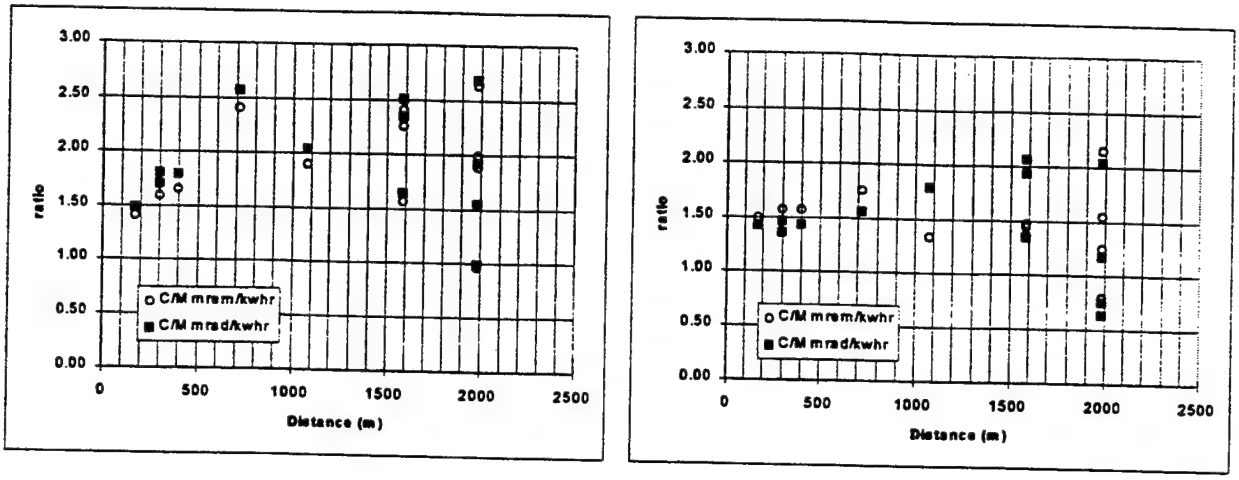

Figure 3-8. Neutron doses and dose equivalents as measured by remmeter, calculation to measurement ratio, as calculated (left) and corrected (right).

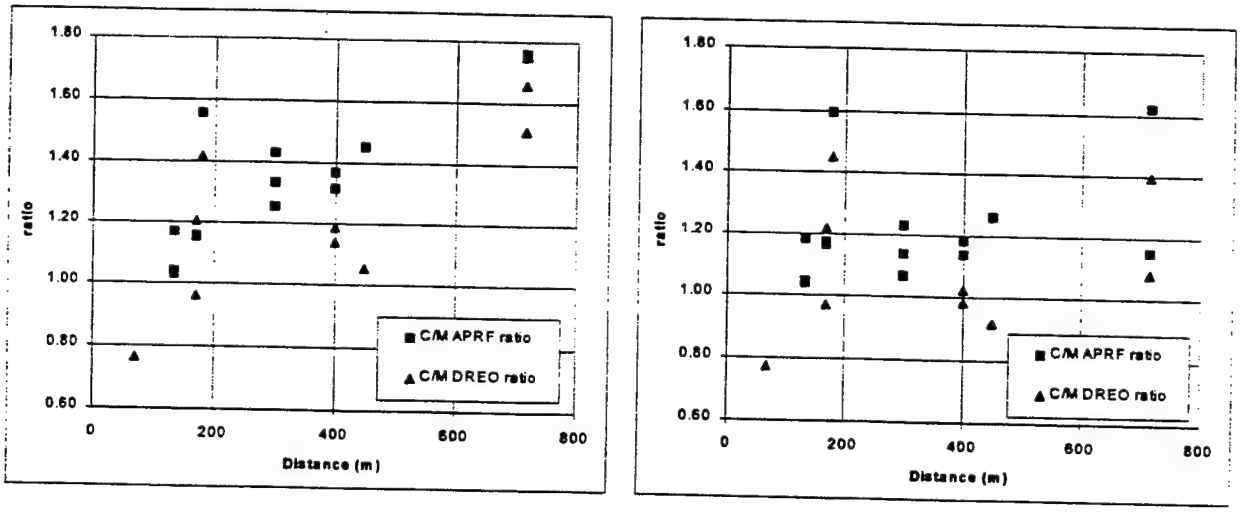

Figure 3-9. Proton recoil (ROSPEC) neutron doses calculation to measurement ratio, calculation to measurement ratio, as calculated (left) and corrected (right).

Figure 3-9 shows the ROSPEC, proton recoil, calculation to measurement ratios, uncorrected and corrected for neutron dose. As in the case of the sulfur, the correction resulted in a substantial improvement, particularly in the case of ground level measurements at 715 meters. The correct calculations are between zero and twenty percent high. This is the same direction as evidenced by the remmeter, but a lesser extent. Little improvement was obtained in the case of measurements made at 30 meters height.

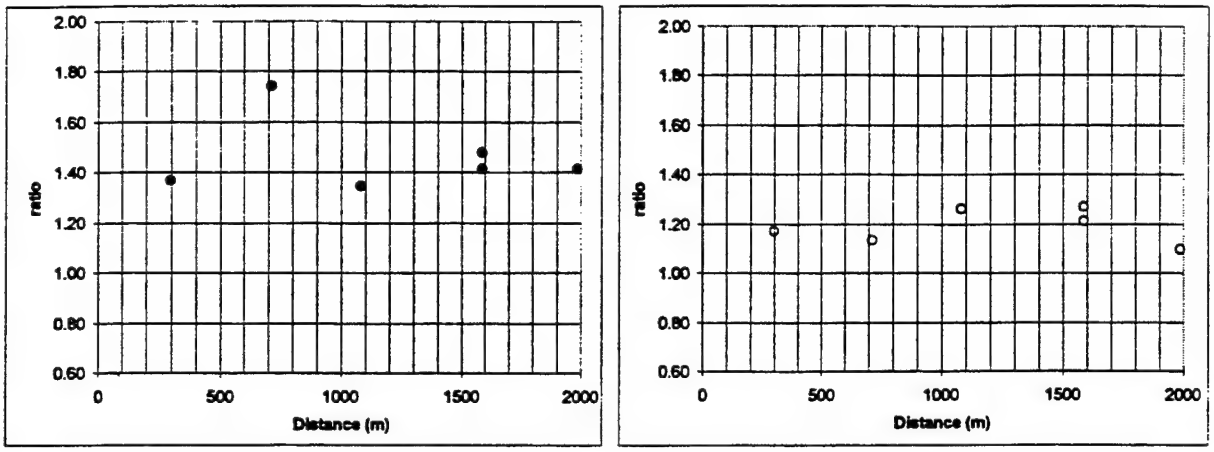

Figure 3-10. Bonner Ball neutron dose calculation to measurement ratio, as calculated (left) and corrected (right).

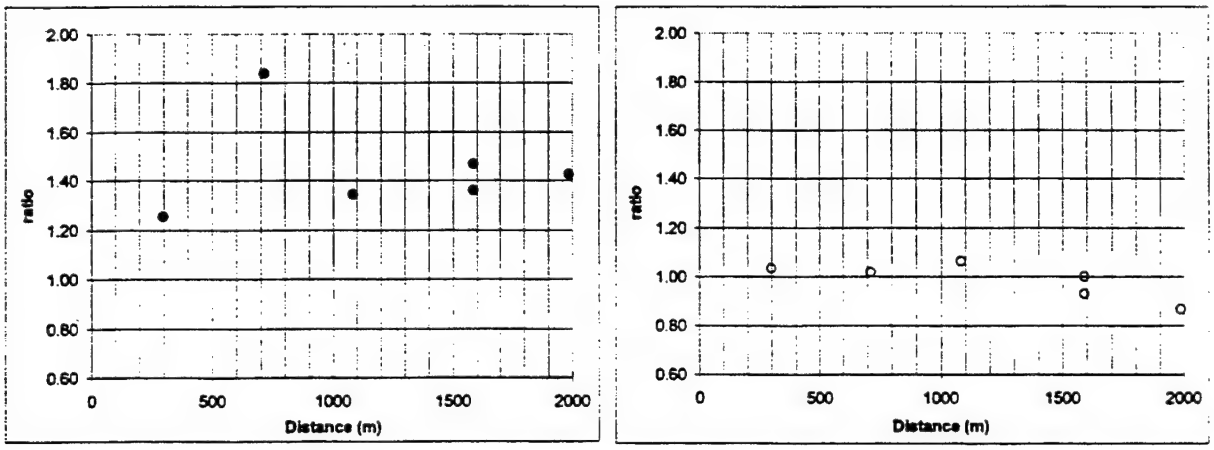

Figure 3-11. Bonner Ball greater than 3 MeV neutron fluence calculation to measurement ratio, as calculated (left) and corrected (right).

Figure 3-10 and 3-11 show the calculation to measurement ratios obtained with the Bonner Balls for neutron dose and fluence greater than 3 MeV (sulfur fluence), respectively. The corrected calculations compare to the Bonner Ball dose measurements in a manner very similar to that obtained for ROSPEC, i.e., on the order of twenty percent higher. The Bonner Ball greater than 3 MeV neutron fluence measurement (Figure 3-11) is quite consistent with the ground level sulfur data and, further, takes that agreement out to two kilometers.

Finally, Figure 3-12 shows the uncorrected and corrected comparisons for the case of the boron-loaded plastic scintillator. The correction gains some improvement in the case of the neutron dose. However, the greatest improvement is in the case of the greater than 3 MeV fluence, where the corrected calculations agree with the measurements within approximately ten percent.

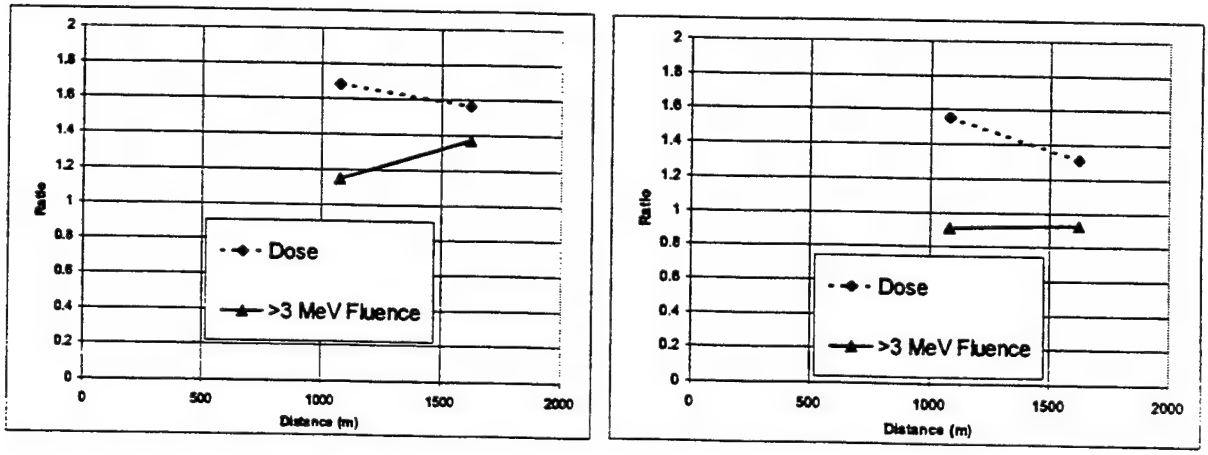

Figure 3-12. Boron-loaded plastic scintillator dose and fluence (>3 MeV) calculation to measurement ratio, as calculated (left) and corrected (right).

SECTION 4
LUCITE PHANTOM SHIELDING CALCULATIONS

Thermal neutron fluence distributions were measured in a cylindrical acrylic phantom, borrowed by APRF from ETCA. Gold foils were placed at various distances in the phantom. The hydrogenous material rapidly scattered the neutrons down to thermal energies. The effect at the center of the phantom was to reduce non-thermal neutrons by an order of magnitude and raise the thermal fluence several times.

A mathematical phantom was constructed to closely represent the actual phantom. The vertical cylinder's length was 21cm; the diameter was 21cm. 5cm diameter discs of material 0.34cm thick were removed from the phantom to represent the spaces the gold foils were placed. These spaces were centered at depths of 1.17, 3.11, 5.05, 6.99, 8.93, 12.07, 15.95, 17.89 and 19.83cm from the surface closest to the reactor and were midway between the top and bottom of the cylinder.

The neutron and gamma-ray cross sections are from the DABL69 library. The constituents are air and lucite. The elemental densities are given for both the materials in the free-field DORT calculation and the local-shield MASH calculation in Table 4-1. The run number given is that having atmospheric properties similar to the actual run and for which calculations were specifically made.

Table 4-1. Lucite phantom elemental constituents.

Elemental Densities (atoms per barn-centimeter)

	Air	Ground		Lucite
Run	240	240/241		
		10%H2O	25%H2O	
		> 500 m	< 500 m	
H	7.35-7	9.88-3	2.47-2	5.77-2
C		1.66-3	1.66-3	3.61-2
N	3.78-5	5.19-5	5.19-5	
O	1.09-5	3.28-2	4.02-2	1.44-2
Na		1.57-4	1.57-4	
Mg		1.00-4	1.00-4	
Al		1.51-3	1.51-3	
Si		1.06-2	1.06-2	
P		0.00	0.00	
S		3.83-6	3.83-6	
Cl		3.76-6	3.76-6	
Ar	2.26-7	2.28-7	2.44-7	
K		2.25-4	2.25-4	
Ca		1.28-3	1.28-3	
Mn		8.01-6	8.01-6	
Fe		3.52-4	3.52-4	
Cu		5.32-7	5.32-7	

The detector is located 125 cm above the ground, in the center of the road and at 2.5m from the edge of the road. It is also placed 30m above the center of the road. For the phantom, detectors were located in each of the inside air spaces.

MASH calculates the local radiation fluences by using the adjoint Monte Carlo method to transport radiation response as a source importance from the detector location out of the shield to produce an adjoint fluence. A companion code, DRC, then is used to fold together the adjoint fluence with the free-field fluences calculated by

DORT. This allows one to calculate the fluence and responses at the detector location in the local shield, which is exposed to the free field fluences at APR. For the tree problem 750,000 particle histories were started. For the phantom problem 50,000 histories were started. These numbers are adequate to calculate the dose and spectra to a statistical uncertainty less than 1% and 5%, respectively.

Figure 4-1 illustrates the calculated neutron thermal fluence distribution from the MASH code, including free field spectra from DORT and spectra calculated inside the lucite phantom, using the DRC code to couple the DORT free field at 170 meters with the MORSE shielding calculations. Three types of fluence information are shown, bare foil activation, cd-covered foil activation and thermal activation. The term "Thermal" refers to cadmium-difference fluence, i.e., the difference between the cadmium-covered and the bare gold foil activation. Thus, the thermal fluence is defined to be that below the so-called cadmium cutoff of 0.414 eV. The actual value is usually given in terms of equivalent 2200 meters per second fluence.

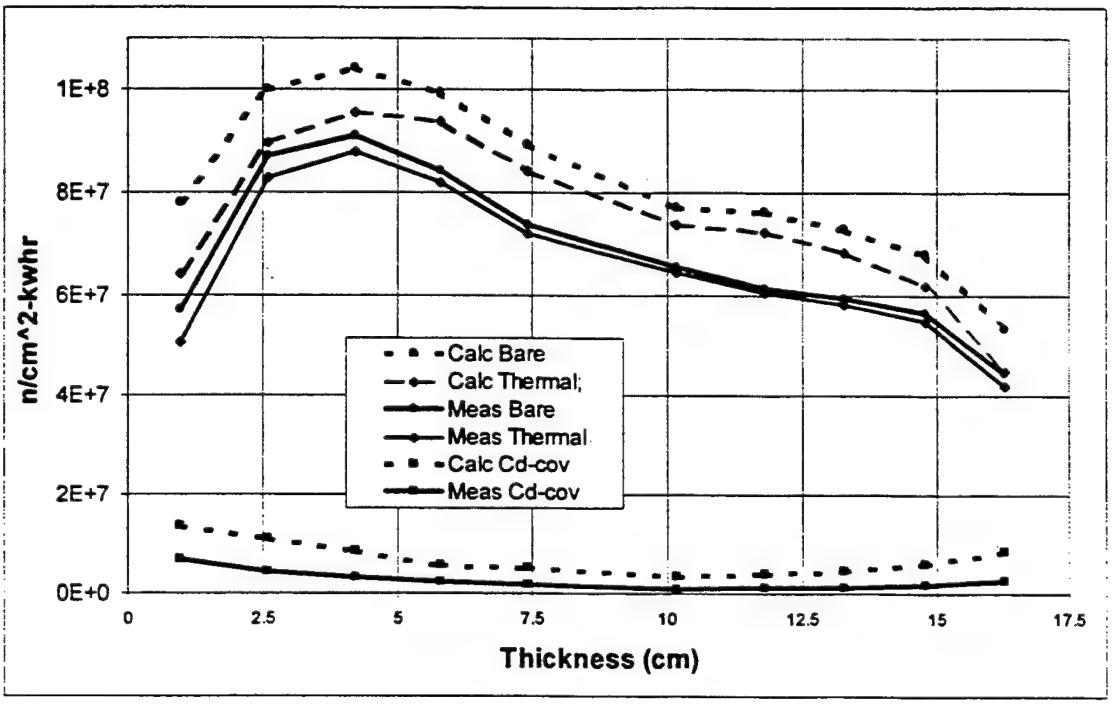

Figure 4-1. Neutron fluence distributions, front to back, in a cylindrical lucite phantom.

Figure 4-2 shows the ratios of calculation to measurement for the three types of information shown in Figure 4-1. The calculated and measured thermal neutron fluence values agree to within approximately 20%. Regrettably, this is not a random difference, but rather it is a bias, with the calculations being consistently higher than the measurements by approximately 20%. Nevertheless, this agreement is very good considering that the DABL69 cross section set has only a single neutron group below 0.414 eV.

The relatively good cadmium-difference fluence agreement between calculations and measurements tends to mask the problems encountered in calculating the epi-cadmium fluence. The coarse energy structure and lack of upscatter in the MASH calculations cause the resonance structure of the gold cross section above the cadmium cutoff not to be adequately accounted for. Fortunately, this is seldom of importance in matters associated with biological or electronic shielding for neutrons.

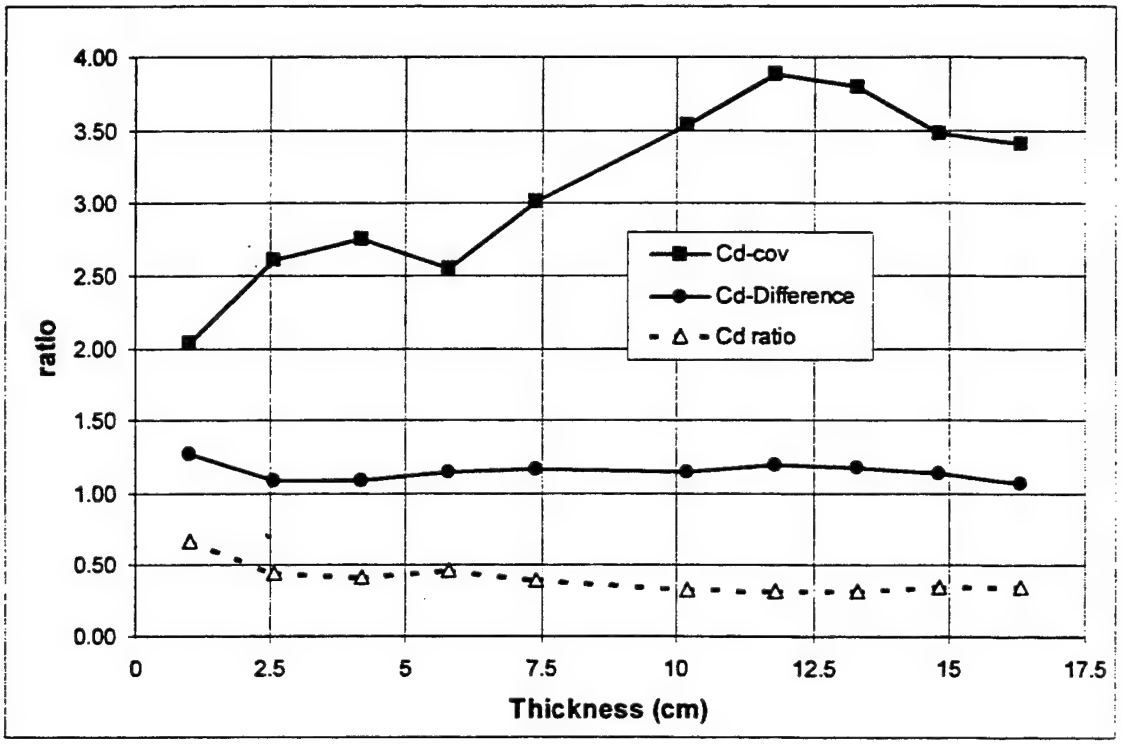

Figure 4-2. Neutron fluence in a lucite phantom, calculation to measurement ratios.

SECTION 5
CONCLUSIONS AND RECOMMENDATIONS

The primary purpose of the REP program is to verify and validate the MASH shielding analysis system for routine application by military services, their laboratories and contractors. The criterion for the certification of MASH is that it must reproduce the measured values to within ± 20% (one standard deviation). The most important quantity for MASH to accurately reproduce is the shielding factor. That quantity is not really tested by the majority of measurements compared to in this report. Rather, it is the ability of MASH components to correctly predict the free field that is the subject here.

Based on the comparisons between MASH free field calculations and measurements in this report, MASH appears capable of matching most of the measured dose values to within approximately twenty percent. This is true of both the neutron and gamma ray doses separately and combined. However, there are some caveats that must be placed on this conclusion. First, care must be taken to include the affect of the foliage surrounding the important measurement locations of 300, 400 and 715 meters and to account for local peculiarities, such as backfilled areas under the detector. This may be done using the tools provided with the MASH system, though not without some considerable effort. Were it not done, the twenty- percent criterion would not appear to be met. Second, the calculation to measurement ratios have values of one hundred and twenty percent for nearly all the measurement types. This places the calculations at the very edge of the acceptance criterion. Finally, comparisons are likely to fall outside of the twenty-percent acceptance range for distances beyond approximately one kilometer, even if local shielding affects are considered. Thus, the following issues are important to the future development of MASH in order that it gain additional reliability for all applications.

The forest at APRF has been shown to reduce neutron kerma approximately 15% to 20% below that attributed to a bare plane, depending on the energy range of interest. The inclusion of the forest in the calculation results in a much more uniform comparison between the neutron dose and fluence calculations and measurements made with all types of detectors. It is largely responsible for enabling MASH neutron calculations to meet the 20% acceptance criterion within one kilometer of the source. However, it does little or nothing to improve the agreement between calculated and measured gamma rays. In demonstrating the importance of the forest effect, these calculations have demonstrated the need for a capability to couple over more than one radial mesh for large problem applications, as well as the need for other, more esoteric corrections for applications in other circumstances, such as in the case of a large geometry, close to the source.

Second, the terrain has little effect on the results except at 170 meters, where it causes a much-needed increase in the gamma ray dose. Thus, even this factor, minor in its overall impact, plays an important part in helping to reconcile the calculations and measurements. Even so, the issue of the effects of large terrain features and their affect on fluence, dose and shielding is an important subject, not truly addressed in REP.

Finally, the use of ENDF/B-VI cross sections has been shown to make important changes in the neutron spectra and kerma. At 400 meters use of ENDF/B-VI shifts fluence downward in energy and increases the calculated kerma. In fact, applied alone, the new cross sections perform the function of making agreement between calculation and measurement worse, so that the additional step of taking the forest into account can make the agreement better. In the case of the APRF source, the primary benefit of ENDF/B-VI cross sections is the accurate calculation of neutron fluence above 3 MeV. Previous cross sections, including the MASH DABL69 set, based on ENDF/B-V, over-predicted the transport of such fluence. This had a cascade affect, causing an ever increasing discrepancy between calculated and measured dose with increasing distance. With the inclusion of ENDF/B-VI cross sections (and proper accounting of terrain and forest effects) virtually all comparisons of calculated and measured dose values shown in this report demonstrate a nearly uniform bias upward of the calculations in the ten to twenty percent range, over all distances. It is not clear whether this residual discrepancy is due to an error in the calculations, i.e., an anomalous buildup of dose producing neutrons below 3 MeV, or due to some aspect of the measurement. It should be noted however that the discrepancy is in evidence to some degree for all types of measurement devices.

SECTION 6
REFERENCES

1 Byrd, R., Estes, G. and Mannon, C., "Far-Field Fast-Neutron Energy Spectra from an Unshielded Fission Reactor, "LA-12870-MS, Los Alamos National Laboratory, Los Alamos, NM, March 1995 (UNCLASSIFIED)

2 Goldhagen, P., Reginatto, M., and Hajnal, F., "Neutron Spectrum Measurements at Distances Up to 2 km from a Uranium Fission Source for Comparison with Transport Calculations," U.S. Dept. of Energy Environmental Measurements Laboratory, New York, NY, in Proceedings of the 1996 Topical Meeting, Radiation Protection and Shielding, American Nuclear Society, Inc., La Grange Park, IL, April 1996. (UNCLASSIFIED)

3 Heimbach, C., Oliver, M., and Stanka, M., "Research Report of the Radiation Transport in Air-Over-Ground Geometry (Summary: 1992-1993)," ATC-7793, Radiation Simulation and Analysis Directorate, U.S. Army Aberdeen Test Center, Aberdeen Proving Ground, MD, December 1995. (UNCLASSIFIED)

4 Johnson, J., "A User's Manual for MASH 1.0 - A Monte Carlo Adjoint Shielding Code System," ORNL/TM-11778, Oak Ridge National Laboratory, Oak Ridge, TN, March 1992. (UNCLASSIFIED)

5 Kaul, D. C., and Egbert, S. D., "Radiation Leakage from the Army Pulse Radiation Facility (APRF) Fast Reactor," SAIC-89/1423, Draft Report submitted to U.S. Army Combat Systems Test Activity, Aberdeen Proving Ground, MD by Science Applications International Corporation, San Diego, CA, 1989. (UNCLASSIFIED)

6 Kaul, D., C., Egbert, S. D. and Roberts, J., "FY90 Radiation Environment Program (REP)," SAIC-91-1051, Radiation Simulation and Analysis Directorate, U.S. Army Aberdeen Test Center, Aberdeen Proving Ground, MD, March 1991. (UNCLASSIFIED)

7 Kerr, G. D., "Photon and Neutron Fluence-to-Kerma Conversion Factors for ICRP-1975 Reference Man Using Improved Elemental Compositions for Bone and Marrow of the Skeleton," ORNL/TM-8318, Oak Ridge National Laboratory, Oak Ridge, TN, 1982. (UNCLASSIFIED)

8 Santoro, R., and Whitaker, S., "DNA Radiation Environments Program, Spring 1990 2-Meter Box Experiments and Analyses," ORNL/TM-12160, Oak Ridge National Laboratory, Oak Ridge, TN, September 1992. (UNCLASSIFIED)

9 Straume T., Harris, L., Marchetti, A., and Egbert, S., "Neutrons Confined in Nagasaki and at the Army Pulsed Radiation Facility: Implications for Hiroshima," Radiation Research 138: 193-200, 1994. (UNCLASSIFIED)

APPENDIX A
REACTOR RUNS, METEOROLOGICAL AND SURFACE CONDITIONS, 1992 - 1994
MEASUREMENT SERIES

A.1 REACTOR RUNS.

Reactor runs for REP program measurements, 1992 through 1994. Of the thirty reactor runs, calculations were performed for nine. The second column (Calc. As) gives the calculated run number and its association with an actual run.

Run Number	Calc. As	date	reactor operating time			subinterval time			Energy KWHR
			Start	End	Duration	Start	End	Duration	
		3/23/92							
SS92-066	66	3/24/92	11:35:30	17:57:30	6:22:00				50.0000
		3/25/92							
		5/26/97							
SS92-154	157	5/27/92	11:59:00	16:12:00	4:13:00				37.5400
SS92-155	240	5/27/92	17:12:07	17:17:07	0:05:00				0.0004
SS92-156	157	5/28/92	10:00:35	10:14:35	0:14:00				0.0008
SS92-157	157	5/28/92	11:24:00	12:04:00	0:40:00				50.0000
SS92-158	241	5/29/92	10:22:00	12:00:00	1:38:00				0.8458
SS92-186	228	6/17/92	10:00:33	11:31:33	1:31:00				12.0000
SS92-210	76	7/7/92	9:57:10	16:12:10	6:15:00				50.0000
SS92-228	228	8/24/92	13:20:41	14:30:00	1:09:19				0.5777
SS92-229	76	8/24/92	15:26:45	16:48:45	1:22:00				0.0683
SS92-230	228	8/25/92	9:46:22	11:05:22	1:19:00				0.1317
SS92-231	231	8/25/92	13:06:14	14:21:14	1:15:00				3.7500
SS92-232	231	8/25/92	15:23:41	15:53:41	0:30:00				1.5000
SS92-233	231	8/26/92	10:05:42	12:05:42	2:00:00				2.0000
SS92-234	236	8/26/92	13:38:54	14:56:54	1:18:00				1.9500
SS92-235	231	8/27/92	9:51:20	11:03:20	1:12:00				1.8000
SS92-236	236	8/27/92	12:53:45	14:11:45	1:18:00				0.6500
SS92-237	236	8/27/92	14:58:19	15:17:19	0:19:00				0.0158
SS92-238	231	8/28/92	9:52:03	11:09:03	1:17:00				0.2567
SS92-239	77	8/31/92	14:42:51	15:57:51	1:15:00				0.0250
SS92-240	240	9/1/92	11:32:28	15:17:28	3:45:00				26.2500
SS92-241	241	9/2/92	9:49:06	13:49:06	4:00:00				28.0000
SS92-242	228	9/3/92	13:18:31	14:18:31	1:00:00				3.0000
SS93-071	240	6/14/93	12:39:49	13:44:49	1:05:00				0.0068
SS93-072	77	6/14/93	15:34:35	16:35:00	1:00:25	15:40:00	16:30:00	0:50:00	0.0201
SS93-073	77	6/15/93	10:24:38	11:24:38	1:00:00				1.0000
SS93-074	76	6/15/93	12:12:16	16:11:46	3:59:30	12:16:00	16:10:00	3:54:00	30.3800
SS93-075	240	6/16/93	9:25:35	11:33:00	2:07:25	9:30:00	11:33:00	2:03:00	15.9300
SS93-076	76	6/17/93	9:15:57	12:02:27	2:46:30	9:19:00	12:03:00	2:44:00	20.8100
SS93-077	77	6/17/93	12:51:25	16:42:08	3:50:43	13:17:00	16:40:00	3:23:00	28.8400

A.2 METEOROLOGICAL CONDITIONS.

Meteorological measurements made at the Spesutie Island observation site. All observations pertain to sea level.

Run Number	date	ATM time	ATM Pres in Hg	Temp deg f	Rel Hum %	ATM Pres mbar	Temp deg c
SS92-066	3/23/92 3/24/92 3/25/92	14:00:00	30.238	44.00	31	1023.98	6.67
	5/26/97						
SS92-154	5/27/92	13:00:00	29.930	63.50	71	1013.55	17.50
SS92-155	5/27/92	17:00:00	29.919	66.7	47	1013.17	19.28
SS92-156	5/28/92	10:00:00	30.128	65.1	56	1020.25	18.39
SS92-157	5/28/92	11:00:00	30.134	67.60	49	1020.45	19.78
SS92-158	5/29/92	10:00:00	30.274	68.80	64	1025.20	20.44
SS92-186	6/17/92	12:00:00	30.280	76.80	69	1025.40	24.89
SS92-210	7/7/92	12:00:00	30.056	78.40	58	1017.81	25.78
SS92-228	8/24/92	14:00:00	30.238	80.30	72	1023.98	26.83
SS92-229	8/24/92	16:00:00	30.214	81.60	59	1023.16	27.56
SS92-230	8/25/92	10:00:00	30.176	79.60	86	1021.88	26.44
SS92-231	8/25/92	14:00:00	30.132	87.30	75	1020.39	30.72
SS92-232	8/25/92	16:00:00	30.103	86.10	78	1019.40	30.06
SS92-233	8/26/92	11:00:00	30.086	83.20	76	1018.83	28.44
SS92-234	8/26/92	14:00:00	30.031	89.10	60	1016.97	31.72
SS92-235	8/27/92	10:00:00	29.958	85.10	79	1014.49	29.50
SS92-236	8/27/92	14:00:00	29.889	89.50	64	1012.16	31.94
SS92-237	8/27/92	15:00:00	29.864	89.90	62	1011.31	32.17
SS92-238	8/28/92	11:00:00	29.730	83.30	82	1006.77	28.50
SS92-239	8/31/92	15:00:00	29.938	81.30	39	1013.82	27.39
SS92-240	9/1/92	13:00:00	30.108	75.50	51	1019.57	24.17
SS92-241	9/2/92	12:00:00	30.174	70.60	76	1021.81	21.44
SS92-242	9/3/92	14:00:00	29.990	77.60	85	1015.58	25.33
SS93-071	6/14/93	12:00:00	30.108	76.40	48	1019.57	24.67
SS93-072	6/14/93	15:00:00	30.072	80.30	40	1018.36	26.83
SS93-073	6/15/93	10:00:00	30.009	73.70	80	1016.22	23.17
SS93-074	6/15/93	13:00:00	29.965	79.10	64	1014.73	26.17
SS93-075	6/16/93	10:00:00	30.116	76.60	55	1019.85	24.78
SS93-076	6/17/93	10:00:00	30.210	78.90	56	1023.03	26.06
SS93-077	6/17/93	14:00:00	30.172	85.60	34	1021.74	29.78

A.3 GROUND MOISTURE CONDITIONS.

All data were taken using the Seaman Nuclear Moisture/Density meter (SOP 385-304). The meter records bulk density and dry density in pounds per cubic foot and pertain to the mean value over 6 inches of soil depth. Meter values have been interpreted into ground moisture content in terms of water content as a percent of dry soil density.

Run Number	Dist. (m): date	135	170	300	400	450	715	1080	1600	2000
	3/23/92	38.32	31.06	81.71	49.17	42.33	35.50			
SS92-066	3/24/92		38.26							
	3/25/92	33.93	29.47	62.88	44.76	59.47	26.51			
	5/26/97	23.21	21.46	35.23	22.03	33.76				
SS92-154	5/27/92		32.79		25.07				28.89	
SS92-155	5/27/92									
SS92-156	5/28/92									
SS92-157	5/28/92									
SS92-158	5/29/92	25.19	19.00	29.53	23.06	38.07	18.66	10.70	13.56	22.76
SS92-186	6/17/92	13.34	21.33							
SS92-210	7/7/92	22.44	22.09	22.04	18.16	32.00				
SS92-228	8/24/92	24.18	21.37	21.69	21.32	33.82				
SS92-229	8/24/92	24.18	21.37	21.69	21.32	33.82				
SS92-230	8/25/92	25.98			5.48g					
SS92-231	8/25/92	25.98			5.48g					
SS92-232	8/25/92	25.98			5.48g					
SS92-233	8/26/92									
SS92-234	8/26/92									
SS92-235	8/27/92			17.34	3.787g	29.78				
SS92-236	8/27/92			17.34	3.787g	29.78				
SS92-237	8/27/92			17.34	3.787g	29.78				
SS92-238	8/28/92									
SS92-239	8/31/92	35.52	22.40	20.18	4.682g					
SS92-240	9/1/92						9.80			
SS92-241	9/2/92						10.08			
SS92-242	9/3/92				6.72					
SS93-071	6/14/93		16.52	39.56					8.55	13.97
SS93-072	6/14/93		16.52	39.56					8.55	13.97
SS93-073	6/15/93		14.58	38.47					9.25	11.80
SS93-074	6/15/93		14.58	38.47					9.25	11.80
SS93-075	6/16/93								9.12	8.88
SS93-076	6/17/93									
SS93-077	6/17/93		12.83	29.08					6.68	11.21

APPENDIX B
MEASURED AND CALCULATED FLUENCE, 1992 - 1994 MEASUREMENT SERIES

This appendix contains representative measured and calculated neutron fluence selected from the ROSPEC and boron-loaded scintillator measurements between 1992 and 1994. The Calculations correspond to the basic MASH system, as of April 1992 with the 1990 APRF source update. Combined ENDF/B-6 cross section, terrain and forest effects are also shown.

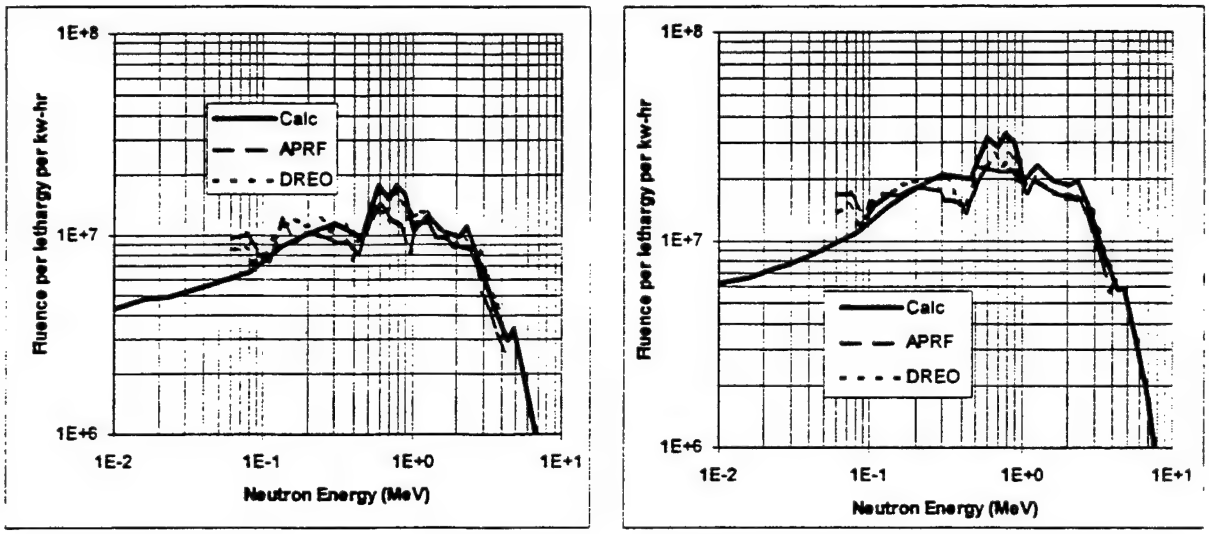

Figure B-1. Neutron fluence, run SS92-228 at 170m distance, uncorrected (left) and corrected (right).

At 135 meters there is little distance for transport to take place, except below approximately one MeV, where scattering from the ground and in the air can cause a buildup of fluence. According to Figure B-1, the calculations agree with the measurements in the fast neutron region above one MeV, but overpredict the buildup below that energy. Similar results are obtained comparing spectra at greater distances.

At 400 meters the measurements are in the middle of the 40 meter-wide corridor of trees that begins approximately half way from the reactor. Figure B-2 shows the measured fluence at 400 meters, compared to calculations, uncorrected and corrected. . The uncorrected fluence is much larger than the measurements in the 1 to 3 MeV regime, as well as the 400 keV to 1 MeV regime. The corrections cause the regime above 1 MeV to show good agreement between calculation and measurement. However, the regime below 1 MeV shows the calculations to be somewhat high compared to the measurements. At 400 meters it is not expected that the switch from ENDF/B-V to ENDF/B-VI cross sections will have a very large effect on the results. Therefore, it is assumed that most of this correction is due to accounting for terrain and forest.

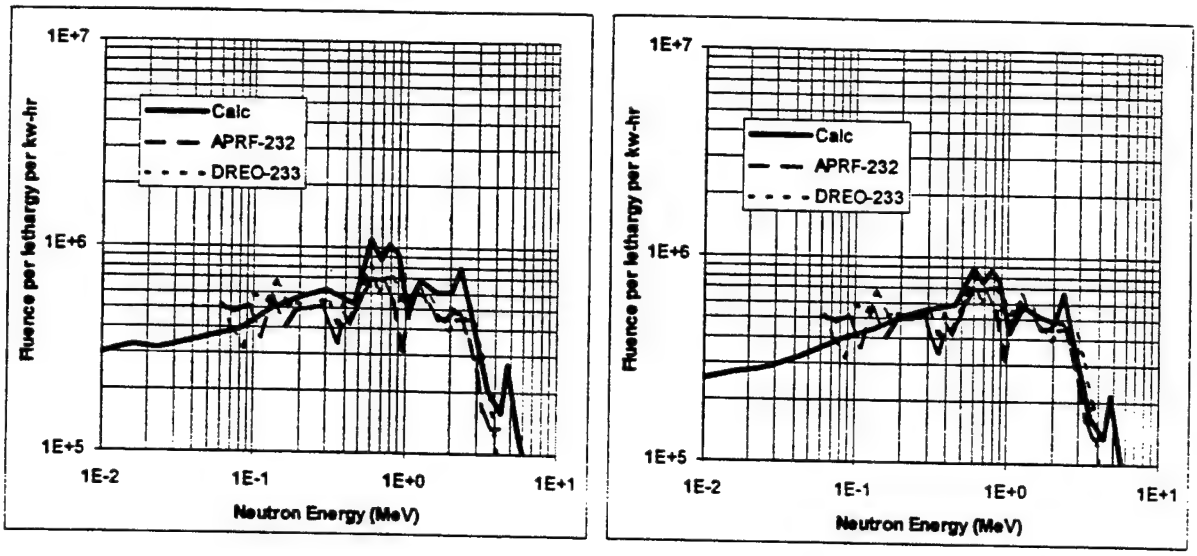

Figure B-2. Neutron fluence, runs SS92-232 and 233 at 400m distance, uncorrected (left) and corrected (right).

At 715 meters the measurement takes place on a road in the middle of a forest, and the road is at an angle of approximately 45 degrees to the line-of-sight to the reactor. Figure B-3 shows the effect of the forest alone. As note in the body of the report, the calculated fluence is very sensitive to the postulated width of the cleared area. The values shown are for a 30 meter wide corridor. The affect of the forest is to dramatically improve the calculation to measurement comparison. The effect of the change in cross sections is to improve the calculation/measurement agreement above 1 MeV. However, the calculations remain higher than the measurements in the energy regime between approximately 400 keV and 1 MeV.

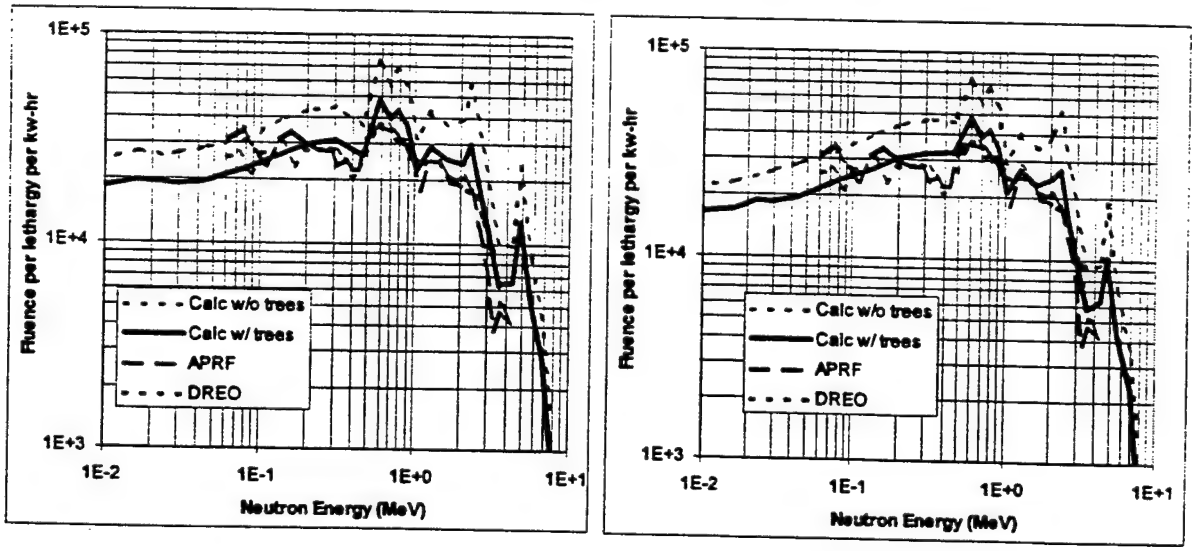

Figure B-3. Neutron fluence, Run SS92-240 at 715m distance (on road), uncorrected (left) and corrected (right).

At 1080 meters the measurements are made near the top of a sandy knob of dirt, constructed to test the climbing power of military vehicles. There is no clear line-of-sight to the reactor, nor is there any significant amount of foliage in the immediate vicinity of the measurement. Therefore, the correction applied to the calculation is strictly due to the substitution of ENDF/B-VI cross sections. It can be seen in Figure B-4 that the effect of the correction is to reduce the high energy neutron fluence. Little correction is seen in fluence below approximately 2 MeV, where the calculations are consistently larger than the measurements. This discrepancy is particularly large below 1 MeV, a range in which the calculations are consistently higher than the measurements at all distances.

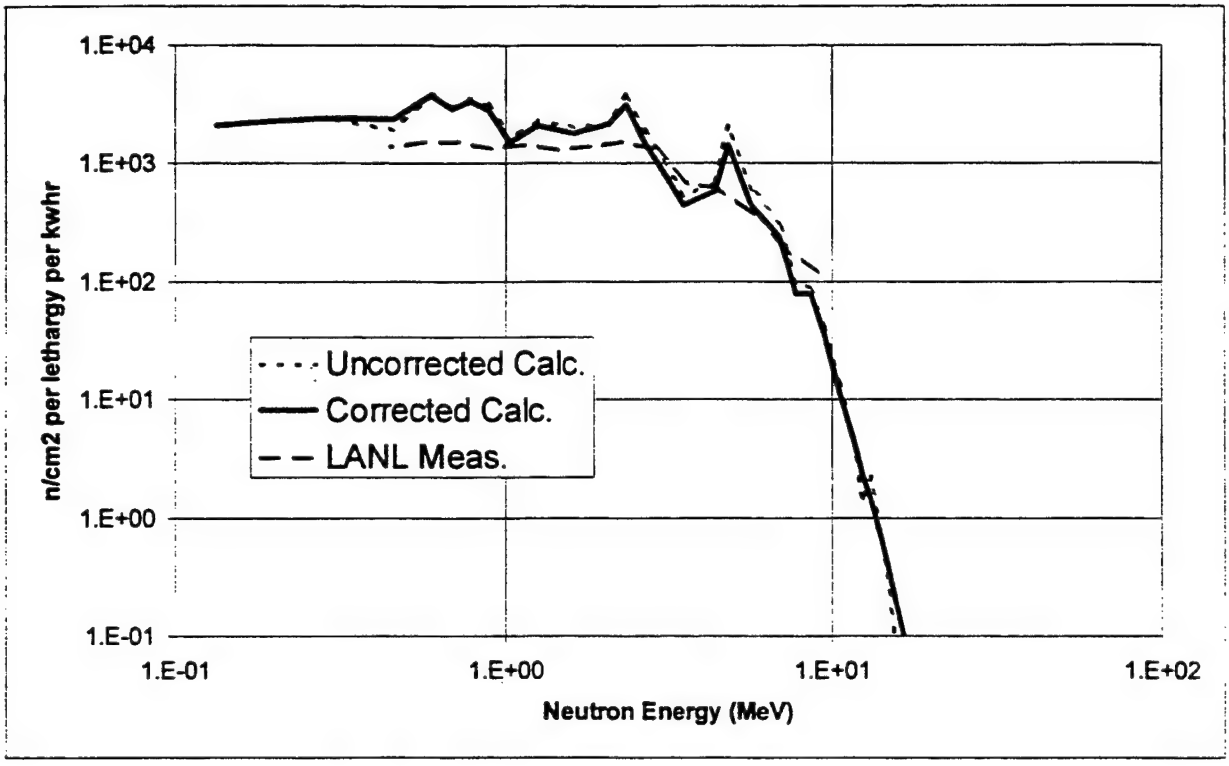

Figure B-4. Neutron fluence, 1080 meters.

At 1600 meters the measurements are made on flat ground at the obstacle course near the entrance to the APRF facility. There is no clear line-of-sight to the reactor, nor is there any significant amount of foliage within fifty meters of the measurement, particularly in the direction of the reactor. Again, the correction applied to the calculation is strictly due to the substitution of ENDF/B-VI cross sections. It can be seen in Figure B-5 that the effect of the correction is to reduce the high energy neutron fluence, above approximately 3 MeV. Unlike 1080 meters, some correction is seen in fluence below approximately 2 MeV, even so the calculations are consistently larger than the measurements in that energy regime. Again, this discrepancy is particularly large below 1 MeV, a range in which the calculations are consistently higher than the measurements at all distances.

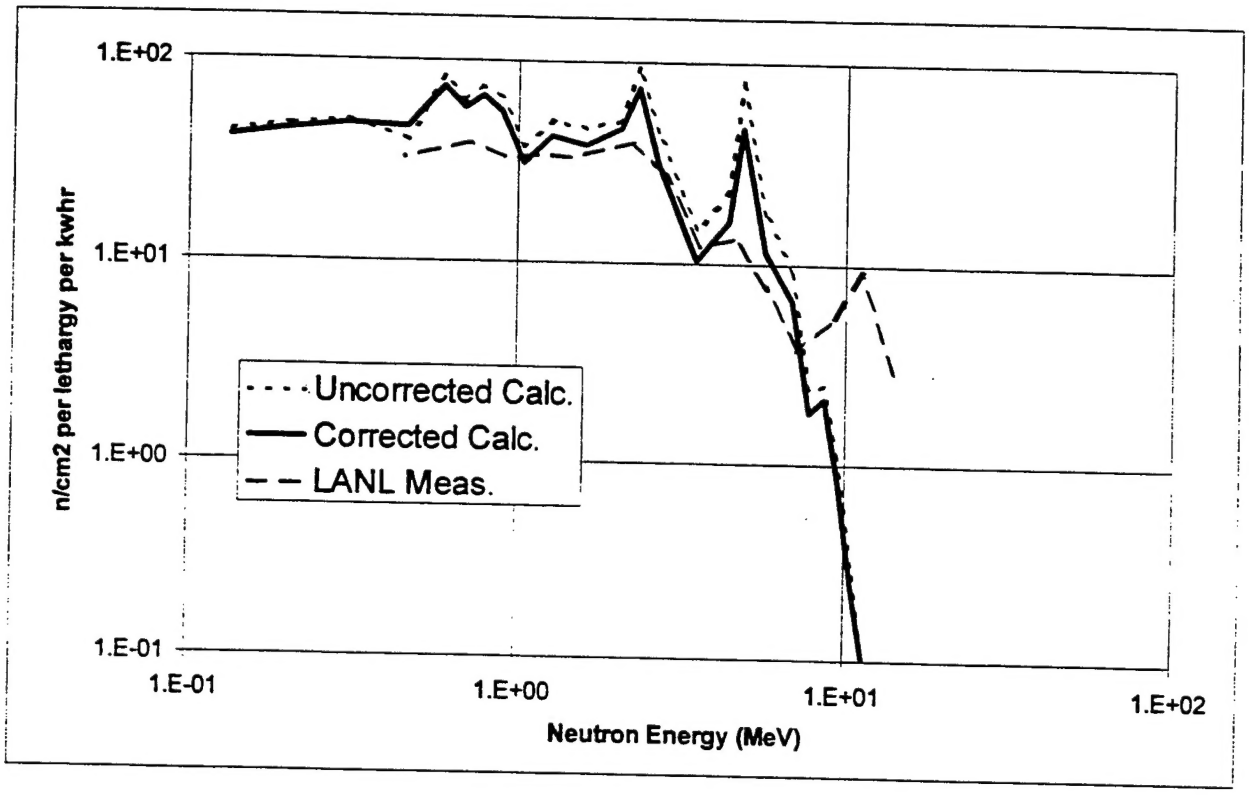

Figure B-5. Neutron fluence, 1600 meters.

DISTRIBUTION LIST

DEPARTMENT OF DEFENSE

DIRECTOR
ARMED FORCES RADIOBIOLOGY RSCH INST
INFORMATION SERVICES DEPARTMENT
8901 WISCONSIN AVENUE
BETHESDA, MD 20889-5603
ATTN: MRA
ATTN: TECHNICAL LIBRARY

ASSISTANT SECRETARY OF DEFENSE
(INTERNATIONAL SECURITY POLICY)
ROOM 4E814, THE PENTAGON
WASHINGTON, DC 20301-2600
ATTN: NUCLEAR FORCES & ARMS
CONTROL POLICY

DEFENSE TECHNICAL INFORMATION CENTER
8725 JOHN J. KINGMAN ROAD, SUITE 0944
FORT BELVOIR, VA 22060-6218
ATTN: DTIC/OCP

DEFENSE THREAT REDUCTION AGENCY
6801 TELEGRAPH ROAD
ALEXANDRIA, VA 22310-3398
ATTN: CPW, C. MCFARLAND
ATTN: CPWB
ATTN: CPWPT
ATTN: NS
ATTN: NSE
ATTN: NSS
ATTN: NSSN

PRESIDENT
NATIONAL DEFENSE UNIVERSITY
FORT LESLEY J. MCNAIR
WASHINGTON, DC 20319-6000
ATTN: ICAF, TECHNICAL LIBRARY
ATTN: STOP 315, LIBRARY

DIRECTOR
NET ASSESSMENT
OFFICE OF THE SEC OF DEFENSE
ROOM 3A930, THE PENTAGON
WASHINGTON, DC 20301
ATTN: DOCUMENT CONTROL

HEADQUARTERS
US EUROPEAN COMMAND
UNIT 30400 BOX 1000
APO AE 09128
ATTN: ECJ-3
ATTN: ECJ2-O-T
ATTN: ECJ5-N
ATTN: ECJ5D

COMMANDER
US EUROPEAN COMMAND/ECJ-6-DT
APO NEW YORK 09128-4209
ATTN: ECJ-6

USSTRATCOM/J531T
901 SAC BOULEVARD, SUITE BB11
OFFUTT AFB, NE 68113-5160
ATTN: J-521

DEPARTMENT OF DEFENSE CONTRACTORS

ARES CORPORATION
1800 NORTH KENT STREET, SUITE 1230
ARLINGTON, VA 22209
ATTN: A. DEVERILL

INSTITUTE FOR DEFENSE ANALYSES
1801 N. BEAUREGARD STREET
CONTROL & DISTRIBUTION
ALEXANDRIA, VA 22311
ATTN: D. SCHULTZ

ITT INDUSTRIES
ITT SYSTEMS CORPORATION
ATTN: AODTRA/DTRIAC
1680 TEXAS STREET, SE
KIRTLAND AFB, NM 87117-5669
ATTN: DTRIAC
ATTN: DTRIAC/DARE

JAYCOR
1410 SPRING HILL ROAD, SUITE 300
MCLEAN, VA 22102
ATTN: DR C. P. KNOWLES

PACIFIC-SIERRA RESEARCH
OPERATING COMPANY OF VERID
29801 28TH STREET, 2ND FLOOR
SANTA MONICA, CA 90405
ATTN: G. ANNO

PACIFIC-SIERRA RESEARCH CORPORATION
WASHINGTON OPERATIONS
1400 KEY BOULEVARD, SUITE 700
ARLINGTON, VA 22209
ATTN: G. MCCLELLAN

SCIENCE APPLICATIONS INT'L
CORPORATION
10260 CAMPUS POINT DRIVE
SAN DIEGO, CA 92121-1578
ATTN: D. KAUL, MS 33
ATTN: E. SWICK, MS 33
ATTN: S. EGBERT

DEPARTMENT OF DEFENSE CONTRACTORS

SCIENCE APPLICATIONS INT'L CORPORATION
P. O. BOX 1303
MCLEAN, VA 22102
ATTN: J. MCGAHAN

SCIENCE APPLICATIONS INT'L CORPORATION
P. O. BOX 1374
BELLVIEW, NE 68005-1374
ATTN: R. CRAVER

DEPARTMENT OF ENERGY

DEPARTMENT OF ENERGY
OAK RIDGE NATIONAL LABORATORY
X-10 LABORATORY RECORDS DEPT.
P. O. BOX 2008
OAK RIDGE, TN 37831-6363
ATTN: G. KERR, MS 6480
ATTN: J. PACE, MS 6363
ATTN: J. WHITE, MS 6362

UNIVERSITY OF CALIFORNIA
LAWRENCE LIVERMORE NATIONAL LABORATORY
P. O. BOX 808
LIVERMORE, CA 94551-9900
ATTN: Z. DIVISION LIBRARY

LOS ALAMOS NATIONAL LABORATORY
P. O. BOX 1663
LOS ALAMOS, NM 87545
ATTN: CIC-14: REPORT LIBRARY

SANDIA NATIONAL LABORATORIES
ATTN: MAIL SERVICES
P. O. BOX 5800
ALBUQUERQUE, NM 87185-0459
ATTN: TECHNICAL LIBRARY, MS 0899

DEPARTMENT OF THE AIR FORCE

HEADQUARTERS
AIR COMBAT COMMAND
204 DODD BOULEVARD SUITE 226
LANGLEY AFB, VA 23665-2777
ATTN: ACC/DRPW, LT COL D. LOEWER

AIR UNIVERSITY LIBRARY
600 CHENNAULT CIRCLE
BUILDING 1405, ROOM 160
MAXWELL AFB, AL 36112-6424
ATTN: LIBRARY

ASSISTANT CHIEF OF STAFF
STUDIES AND ANALYSES AGENCY
1570 AIR FORCE PENTAGON
WASHINGTON, DC 20330
ATTN: AFSAA/SAMI

DIRECTORATE OF NUCLEAR
AND COUNTERPROLIFERATION
DEPARTMENT OF THE AIR FORCE
WASHINGTON, DC 20330
ATTN: XOOSS

HQ 497 IG/INOT
5113 LEESBURG PIKE, SUITE 600
FALLS CHURCH, VA 22041-3230
ATTN: INT

NATIONAL AIR INTELLIGENCE CENTER
4180 WATSON WAY
WRIGHT-PATTERSON AFB, OH 45433-5648
ATTN: NAIC/GTA

US AIR FORCE ACADEMY
2354 FAIRCHILD DRIVE, SUITE 3A22
USAF ACADEMY, CO 80840-6214
ATTN: LIBRARY

DEPARTMENT OF THE ARMY

DEPARTMENT OF THE ARMY
DEPUTY CHIEF OF STAFF FOR
OPERATIONS AND PLANS
PENTAGON
WASHINGTON, DC 20310-0460
ATTN: DAMO-SWN
ATTN: DAMO-ZXA

COMMANDER
NUCLEAR EFFECTS DIVISION
DEPARTMENT OF THE ARMY
WHITE SANDS MISSILE RANGE, NM 88002-5176
ATTN: STEWS-NE-T

ASSISTANT COMMANDANT
US ARMY ARMOR SCHOOL
FORT KNOX, KY 40121
ATTN: ATSB-CTD

COMMANDANT
US ARMY CHEMICAL SCHOOL
FORT LEONARD WOOD, MO.
ATTN: DOCTRINE

COMMANDER
US ARMY COMBAT SYSTEMS TEST ACTIVITY
ABERDEEN PROVING GROUND, MD 21005-5059
ATTN: C. HEIMBACH

DEPARTMENT OF THE ARMY

COMMANDER
US ARMY COMBAT SYSTEMS TEST ACTIVITY
ABERDEEN PROVING GROUND, MD 21005-5059
ATTN: J. GERDES, CSTA-RSAD/BLG 860
ATTN: M. STANKA

COMMANDANT
US ARMY COMD & GENERAL STAFF COLLEGE
FORT LEAVENWORTH, KS 66027-6900
ATTN: ATZL-SWJ-CA
ATTN: ATZL-SWT-A

US ARMY CONCEPTS ANALYSIS AGENCY
ATTN: CSCA-EN
8120 WOODMONT AVENUE
BETHESDA, MD 20814-2797
ATTN: TECHNICAL LIBRARY

DIRECTOR
US ARMY MATERIEL SYSTEMS
ANALYSIS ACTIVITY
ABERDEEN PROVING GROUND, MD 21005-5071
ATTN: DRXSY-DS

US ARMY MEDICAL RESEARCH AND
DEVELOPMENT COMMAND
FORT DETRICH, BUILDING 722
FREDRICK, MD 21702-5012
ATTN: SGRD-PLE

US ARMY MODEL IMPROVEMENT STUDY
MANAGEMENT AGENCY
SUITE 808 CRYSTAL SQUARE 2
1725 JEFFERSON DAVIS HIGHWAY
ARLINGTON, VA 22202
ATTN: SFUS-MIS

US ARMY NATIONAL GROUND
INTELLIGENCE CENTER
220 7TH STREET, NE
CHARLOTTESVILLE, VA 22901-5396
ATTN: C. WARD, IANGIC-RMT

COMMANDER
US ARMY NUCLEAR & CHEMICAL AGENCY
7150 HELLER LOOP, SUITE 101
SPRINGFIELD, VA 22150-3198
ATTN: MONA-NU

US ARMY RESEARCH LAB
5232 FLEMING ROAD
ABERDEEN PROVING GROUND, MD
21001-5067
ATTN: SLCBR-DD-T (TECH LIB)
ATTN: SLCBR-TB

US ARMY RESEARCH LABORATORIES
2800 POWDER MILL ROAD
ADELPHI, MD 20783-1197
ATTN: TECHNICAL LIBRARY

COMMANDER
US ARMY TEST & EVALUATION COMMAND
BUILDING 860
ABERDEEN PROVING GROUND, MD 21005
ATTN: STECS-NE(70)

DIRECTOR
US ARMY VULNERABILITY/LETHALITY
ASSESSMENT MANAGEMENT OFFICE
ABERDEEN PROVING GROUND, MD
21005-5001
ATTN: AMSLC-VL-NE, DR J. FEENEY

DEPARTMENT OF THE NAVY

CHIEF OF NAVAL OPERATIONS
2000 NAVY PENTAGON
DEPARTMENT OF THE NAVY
WASHINGTON, DC 20350-2000
ATTN: N455

COMMANDANT
MARINE CORPS
DEPARTMENT OF THE NAVY
WASHINGTON, DC 20380-0001
ATTN: CODE PPO

NAVAL RESEARCH LABORATORY
4555 OVERLOOK AVENUE, SW
WASHINGTON, DC 20375-5000
ATTN: CODE 5227, RESEARCH REPORT

PRESIDENT
NAVAL WAR COLLEGE
686 CUSHING ROAD
NEWPORT, RI 02841-1207
ATTN: DOCUMENT CONTROL
ATTN: LIBRARY, CODE 1E22

OFFICE OF NAVAL INTELLIGENCE
4251 SUITLAND ROAD
WASHINGTON, DC 20395-5720
ATTN: NTIC-DA30